generate patient-specific disease models, now we can use iPS cells.

Long QT syndrome is one of the most common fatal cardiac arrhythmic disorders[5]. Recent molecular and electrophysiological examination established the fundamental disease concepts. But there is no definitive therapy invented so far. Here again, one of the most important points in drug discovery is to generate excellent disease models. Current experimental models for arrhythmic disorders mostly depend on animal model and heterologous expression system in human non-cardiomyocytes or non-human cardiomyocytes. The long QT syndrome type 2 (LQT2) is one of the most common genetic variants in long QT syndrome, and accounts for approximately 40% of genotyped patients[9]. LQT2 is caused by mutation of a potassium channel gene, *hERG* (human ether-a-go-go related gene), now referred to *KCNH2*. To generate the physiological cardiac action potential in human cardiomyocytes, in addition to inward sodium and calcium currents, several potassium currents are notably involved. The inward-rectifier background current (*I*K1), the rapidly activating and inactivating transient outward current (*I*to), and the ultrarapid (*I*Kur), rapid (*I*Kr), and slow (*I*Ks) components of delayed rectifier currents. Those potassium currents have pivotal roles in electrophysiological homeostasis in human cardiomyocytes and the mutations in potassium current genes result in several human arrhythmic disorders. *KCNH2* encodes the a-subunit of the *I*Kr channel, and membrane depolarization induced by strong inward currents produces a sequence of conformation changes within the channel that allows permeation of potassium ions. As a clinical phenotype, LQT2 is likely to result in cardiac events during exercise or emotional stress in more than half cases and during rest or sleep in some cases. More specifically, an auditory stimulus (telephone, alarm clock, ambulance siren, etc) can be a specific trigger in LQT2[10]. β-blocker use significantly reduces the risk of cardiac arrhythmic events in LQT2. And maintenance of the extracellular potassium concentration by long-term oral potassium supplementation is also reported to be effective because it shortens the QT interval in LQT2 patients. Besides those therapies, we cannot fully prevent sudden cardiac death in LQT2 patients. So we have to carry on the drug development for LQT2 by using LQT2 disease model.

In this study we showed the generation of iPS cells from a patient with *KCNH2* G603D mutation. These patient-specific iPS cells may contribute to future analysis for disease pathogenesis and drug innovation.

Materials and Methods

Patient consent

All subjects provided informed consent for blood testing for genetic abnormalities associated with hereditary long QT syndrome. The isolation and use of patient somatic cells was approved by the Ethics Committee of Keio University (approval no. 20-92-5) and the Ethics Committee of Tokyo Medical and Dental University (approval no. 2009-27), and was performed only after the patient and the parent had provided written informed consent.

Generation of human iPS cell

Human iPS cells were established from T lymphocytes as described previously[11,12]. Briefly, peripheral blood mononuclear cells (PBMCs) were separated by the centrifugation of heparinized whole blood sample obtained, using a Ficoll-Paque PREMIUM (GE Healthcae) gradient. The mononuclear cells were seeded on the anti-human CD3 antibody (BD Pharmingen)-coated 6-well plates in 2 mL GT-T502 (KOJIN BIO) medium per well, and incubated for 5 to 7 days until the activated T cells reached 80% to 90% confluent. Activated PBMCs were collected and transferred at 1.5×10^6 cells per well to a fresh anti-CD3 antibody coated 6-well plate, and incubated for an additional 24 hours. Then, the solution which contained sendai virus vectors individually carrying each of *OCT3/4*, *SOX2*, *KLF4*, and *c-MYC* were added at 10 MOI. After 24 hours of infection, the medium was changed to fresh GT-T502 medium, and the cells were collected and split at 5×10^4 cells into 10 cm-plates pre-seeded with mouse embryonic fibroblasts (MEFs) at more 24 hours after infection. After an additional 24 hours of incubation, the medium was changed to human iPS cell medium supplemented with 4 ng/mL of bFGF. The cells were cultured for another 20 days. On day 25, ES cell-like colonies were dissociated mechanically and transferred to a 24 well plate on the MEF feeder cells.

iPS cell culture

Human iPS cells were maintained on irradiated MEF feeder cells in human iPS cell culture medium, consisting of 80% DMEM/F12 (Sigma-Aldrich), 20% KO Serum Replacement (Invitrogen), 4 ng/mL basic fibroblast growth factor (bFGF; WAKO), 2 mmol/L L-glutamine (Invitrogen), 0.1 mmol/L non-essential amino acids (Sigma-Aldrich), 0.1 mmol/L 2-mercaptoethanol, 100 U/mL penicillin, and 100 μg/mL streptomycin

(Invitrogen). The human iPS cell medium was changed every 2 days and the cells were passaged using 1 mg/mL collagenase IV (Invitrogen) every 5-7 days. 293FT cells were cultured in DMEM supplemented with 10% FBS (Nichirei Bioscience), 1 × 10^{-4} M non-essential amino acids (NEAA; Sigma-Aldrich), 2 mmol/L L-glutamine (Invitrogen), 100 U/mL penicillin, and 100 μg/mL streptomycin (Invitrogen).

Immunocytochemistry

Immunostaining was used to analyze the expression of pluripotency markers. Cells were placed on a 35 mm glass-bottomed dish (IWAKI) before being fixed with 4% paraformaldehyde for 30 min at 4℃. The cells were then rinsed three times with phosphate-buffered saline (PBS) and permeabilized with 0.2% Triton-X 100 in PBS. The cells were then washed and blocked with Immunoblock (DS Pharma) three times for 5 min each time. Samples were incubated overnight at 4℃ with each of the primary antibodies: anti-NANOG (1:200 dilution; ab21624; Abcam), anti-OCT3/4 (1:100 dilution; sc-5279; Santa Cruz). Following incubation with primary antibodies, samples were incubated at room temperature for 1 h with the following secondary antibodies: Alexa Fluor 488 chicken anti-mouse IgG (1:200 dilution; A21200; Invitrogen), and Alexa Fluor 594 goat anti-rabbit IgG (1:200 dilution; A11037; Invitrogen). After cells had been washed by PBS, samples were mounted using Vectashield Hard Set Mounting Medium with 4′,6′-diamidino-2-phenylindole (DAPI) (Vector Laboratories) for nuclear staining. Images were obtained using a × 10 objective lens (NA = 0.45) on a fluorescence microscope (BZ-9000; Keyence).

Genome sequencing

DNA sequencing was used to confirm the presence of the LQT2 mutation in patient-derived iPSCs. Genomic DNA was isolated using a Gentra Puregene Cell Kit (Qiagen) and the region encoding *KCNH2*, including the mutation, was amplified using polymerase chain reaction (PCR) with the following primer set: 5′-TAGCCTGCATCTGGTACGC-3′ (forward) and 5′-GCCCGCCCCTGGGCACACTCA-3′ (reverse). The PCR product (277 bp) was electrophoresed on a 1% agarose gel and purified using a Wizard SV Gel and PCR Clean-Up System (Promega). The purified PCR product was sequenced with original primers.

Results

Novel *KCNH2* mutation

A 10-year-old man was given surgery for funnel chest, without any symptoms. Before operation, routine surface electrocardiogram (ECG) was recorded (Figure 1A). At that time, QT interval prolongation at ECG was firstly pointed out. The patient had no history of previous syncopal episode, palpitation or other cardiac symptoms. But his mother showed repetitive syncopal episodes at rest, triggered by sudden loud noises such as alarm clock and telephone call. Exercise testing shortened the QT interval and epinephrine challenge induced the QT interval prolongation and the form of polymorphic ventricular tachycardia called torsades de pointes. She underwent the genetic test which showed the novel *KCNH2* G603D (G1808A) mutation. Therefore he also underwent the genotype analysis which also showed the novel *KCNH2* G603D (G1808A) mutation (Figure 1B).

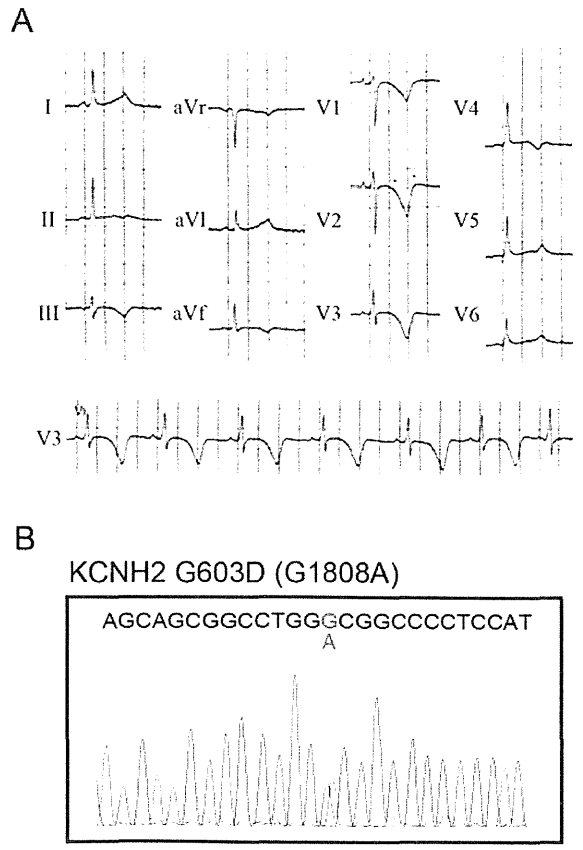

Figure 1. Novel *KCNH2* mutation in the patient.
A. Electrocardiogram from the patient during sinus rhythm. **B.** Sequence analysis of genomic *KCNH2* in the patient. The novel *KCNH2* G603D (G1808A) mutation.

iPS cell generation from a patient with *KCNH2* mutation

To generate iPS cells, we used peripheral blood cells as donor somatic cells from the patient. Separated peripheral mononuclear cells were stimulated by CD3 antibody and IL-2 to activate T lymphocytes. And activated T lymphocytes were reprogrammed by using Sendai virus carrying *SOX2*, *OCT3/4* (also known as *POU5F1*), *KLF4*, and *MYC*. Several clones were generated, expanded and stored. All iPS cell lines showed typical iPS cell morphology and expressed human pluripotency markers (Fig. 2a and b). These iPS cells were moved to petri-dishes and formed embryoid bodies with spontaneous beating, which indicated that these patient-specific iPS cells properly differentiated into beating cardiomyocytes *in vitro*.

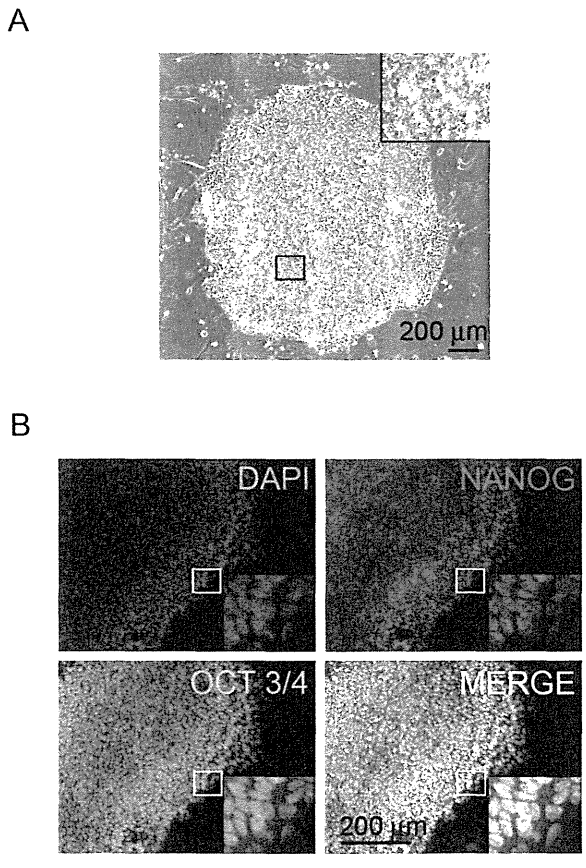

Figure 2. Generation of iPS cells from the patient with *KCNH2* G603D (G1808A) mutation.
A. *Representative phase-contrast image of patient-specific iPS cell colony. Black box in figure is shown at a higher magnification in the inset.* **B.** Immunofluorescence staining for stem cell markers (OCT3/4, NANOG and DAPI) in the patient-specific iPS cell colony. White boxes in each figure are shown at a higher magnification in the inset.

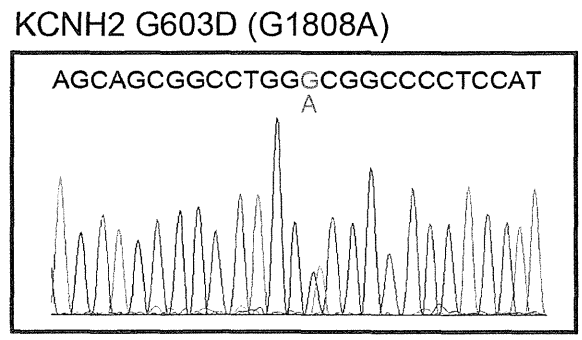

Figure 3. Novel *KCNH2* mutation in the patient-specific iPS cell colony.
Sequence analysis of genomic *KCNH2* in the patient-specific iPS cell colony. The novel *KCNH2* G603D (G1808A) mutation.

KCNH2 mutation in iPS cells derived from a patient with *KCNH2* mutation

To confirm that the generated iPS cells have a same mutation as the patient has, the genotype analysis was performed. It revealed the *KCNH2* G603D (G1808A) mutation was taken over (Figure 3).

Discussion

In the present study, we successfully generated iPS cells from a patient with the *KCNH2* G603D mutation who didn't exhibit any symptoms but showed prolonged QT interval at ECG. This patient is still young and may exhibit the cardiac symptom in the future. In real clinical setting, it is very important to know whether patients with genetic mutation will develop severe diseases or not. If we can predict the severity in the future disease manifestation, we can easily determine to do those patients, e.g., intensive care, exercise limitation, no medication and so on. So it is valuable to establish patient-specific disease model and develop the systems to evaluate the characteristics of patient-specific diseases. Patient-specific iPS cells may contribute to these concepts.

In terms of disease modeling using iPS cells, LQT2 is firstly noticed[13-15] because LQT2 is one of the most common genetic variants in long QT syndrome and there is no definitive therapy for LQT2. And drug discovery often failed at the expense of immense cost, due to the side effects related to HERG which is LQT2 associated gene product, following QT prolongation and lethal arrhythmia. First report showed the generation of LQT2 patient-specific iPS cells harboring A614V missense mutation in the *KCNH2* gene, which was previously shown to lead to a significant reduction of

IKr which is responsible for LQT2[15]. Detailed whole-cell patch-clamp and multi-electrode array (MEA) recordings revealed significant prolongation of the action potential duration in LQT2 iPS cell-derived cardiomyocytes. Voltage-clamp studies confirmed a significant reduction of the cardiac potassium current IKr. LQT2 iPS cell-derived cardiomyocytes also showed marked arrhythmogenicity, characterized by early-after depolarizations (EAD) and triggered arrhythmias. And calcium-channel blockers, K_{ATP}-channel openers and late sodium channel blockers ameliorate the disease phenotype in LQT2 iPS cell-derived cardiomyocyte. Second report showed the generation of LQT2 patient-specific iPS cells harboring G1681A missense mutation in the *KCNH2* gene, which was also previously shown to lead to a significant reduction of IKr[14]. MEA and patch-clamp recording showed prolonged field/action potential duration in LQT2 iPS cell-derived cardiomyocytes. LQT2 iPS cell-derived cardiomyocytes developed EADs when challenged with the E4031 (IKr blocker) and isoprenaline. Action potential duration and EAD were ameliorated by propranolol, nadolol, nicorandil and an activator of hERG, PD118057. The other report showed the generation of LQT2 patient-specific iPS cells harboring R176W missense mutation in the *KCNH2* gene[13]. The *KCNH2* R176W mutation is relatively common variant and was reported to have the frequency of 0.5% in apparently healthy individuals. Although there were some reports showed that this mutation was related to long QT syndrome, the majority of these individuals were completely asymptomatic and unaware of their carrier status, as is the case with this patient. In heterologous expression system, R176W reduced hERG tail current density by ~75%, but upon coexpression with wild type the difference in current densities was nullified. But the action potential duration of LQT2 iPS cell-derived cardiomyocytes was significantly longer than that of control, and IKr density of the LQT2 iPS cell-derived cardiomyocytes was significantly reduced. Consistent with clinical observations, the LQT2 iPS cell-derived cardiomyocytes demonstrated a more pronounced inverse correlation between the beating rate and repolarization time compared with control cells. Additionally, LQT2 iPS cell-derived cardiomyocytes were more sensitive than controls to potentially arrhythmogenic drugs, including sotalol, and demonstrated arrhythmogenic electrical activity.

In this study we chose a patient with a novel mutation in the *KCNH2* G603D. Patient showed QT interval prolongation but never showed any symptoms. To treat properly and prevent cardiac lethal arrhythmia, we believe it is valuable to generate experimental methods to predict how susceptible to lethal arrhythmia in various stimulations in those patients. Actually, many genomic variations such as many SNPs in each patient's genome affect disease manifestation even in the patients with major functional mutation and may be the cause of low penetrance for long QT syndrome[16]. So it is difficult to accurately predict disease susceptibility only by genomic information such as patient's mutation and SNPs. Patient-specific iPS cells have all genomic information encoded in patient's genome including mutation and all SNPs, and can be ideal disease models for the patients. Actually, each patient shows different disease phenotype and drug response, which is also partly due to patient genomic variation. In terms of personalized medicine, we can also try many notorious and beneficial drugs on patient-specific iPS cell-derived cardiomyocyte and predict disease susceptibility before the patient will use those drugs. To generate patient-specific disease models using iPS cells, we established the patient-specific iPS cells and confirmed the patient-specific iPS cells had the same mutation as the patient.

Acknowledgments

The authors thank all the laboratory members for their critical comments and helpful discussions.

References

1. Takahashi K, Yamanaka S. Induction of Pluripotent Stem Cells from Mouse Embryonic and Adult Fibroblast Cultures by Defined Factors. Cell. 2006; 126(4): 663-76.
2. Takahashi K, Tanabe K, Ohnuki M, et al. Induction of Pluripotent Stem Cells from Adult Human Fibroblasts by Defined Factors. Cell. 2007; 131(5): 861-72.
3. Seki T, Yuasa S, Oda M, et al. Generation of Induced Pluripotent Stem Cells from Human Terminally Differentiated Circulating T Cells. Cell Stem Cell. 2010; 7(1): 11-4.
4. Egashira T, Yuasa S, Fukuda K. Induced pluripotent stem cells in cardiovascular medicine. Stem Cells Int. 2011; 2011: 348960.
5. Yuasa S, Fukuda K. Recent advances in cardiovascular regenerative medicine: the induced pluripotent stem cell era. Expert Rev Cardiovasc Ther. 2008 Jul; 6(6): 803-10.
6. Yuasa S, Fukuda K. Cardiac regenerative medicine. Circ J. 2008; 72 Suppl A: A49-55.
7. Egashira T, Yuasa S, Suzuki T, et al. Disease characterization using LQTS-specific induced pluripotent stem cells. Cardiovasc Res. 2012 Sep 1; 95(4): 419-29.
8. Horigome H, Nagashima M, Sumitomo N, et al. Clinical characteristics and genetic background of congenital

long-QT syndrome diagnosed in fetal, neonatal, and infantile life: a nationwide questionnaire survey in Japan. Circ Arrhythm Electrophysiol. 2010 Feb; 3(1): 10-7.
9. Shimizu W, Horie M. Phenotypic manifestations of mutations in genes encoding subunits of cardiac potassium channels. Circ Res. 2011 Jun 24; 109(1): 97-109.
10. Giudicessi JR, Ackerman MJ. Potassium-channel mutations and cardiac arrhythmias—diagnosis and therapy. Nat Rev Cardiol. 2012; 9(6): 319-32.
11. Seki T, Yuasa S, Fukuda K. Generation of induced pluripotent stem cells from a small amount of human peripheral blood using a combination of activated T cells and Sendai virus. Nat Protoc. 2012 Apr; 7(4): 718-28.
12. Seki T, Yuasa S, Fukuda K. Derivation of Induced Pluripotent Stem Cells from Human Peripheral Circulating T Cells. Current Protocols in Stem Cell Biology: John Wiley & Sons, Inc.; 2011.
13. Lahti AL, Kujala VJ, Chapman H, et al. Model for long QT syndrome type 2 using human iPS cells demonstrates arrhythmogenic characteristics in cell culture. Dis Model Mech. 2012 Mar; 5(2): 220-30.
14. Matsa E, Rajamohan D, Dick E, et al. Drug evaluation in cardiomyocytes derived from human induced pluripotent stem cells carrying a long QT syndrome type 2 mutation. Eur Heart J. 2011 Apr; 32(8): 952-62.
15. Itzhaki I, Maizels L, Huber I, et al. Modelling the long QT syndrome with induced pluripotent stem cells. Nature. 2011; 471(7337): 225-9.
16. Priori SG, Schwartz PJ, Napolitano C, et al. Risk stratification in the long-QT syndrome. N Engl J Med. 2003 May 8; 348(19): 1866-74.

Heart Vessels
DOI 10.1007/s00380-013-0324-3

ORIGINAL ARTICLE

Anatomical variations affect radial artery spasm and procedural achievement of transradial cardiac catheterization

Yohei Numasawa · Akio Kawamura · Shun Kohsaka · Masashi Takahashi · Ayaka Endo · Takahide Arai · Yohei Ohno · Shinsuke Yuasa · Yuichiro Maekawa · Keiichi Fukuda

Received: 9 September 2012 / Accepted: 1 February 2013

Abstract Transradial cardiac catheterization (TRCC) has unique technical challenges such as access difficulty related to anatomical variations and/or radial artery (RA) spasm. We sought to evaluate the incidence of anatomical variations of the RA and whether they would affect RA spasm and procedural achievement of TRCC. A total of 744 consecutive patients who underwent TRCC were analyzed by routine radial arteriography. Anatomical variations were defined as abnormal origin of the RA and/or radioulnar loop and/or tortuous configuration. RA spasm was defined as >75 % stenosis at first radial arteriography. Overall, anatomical variations were noted in 68 patients (9.1 %), including 39 cases of abnormal origin (5.2 %), 11 cases of radioulnar loop (1.5 %), and 42 cases of tortuous configuration (5.6 %). Transradial procedures failed in 26 patients (3.5 %), and more frequently in patients with anatomical variation than in those with normal anatomy (23.5 % vs 1.5 %, $P < 0.001$). Importantly, on multivariate analysis the presence of anatomical variation was a distinct predictor of transradial procedure failure (odds ratio (OR) 17.80; 95 % CI 7.55–43.73; $P < 0.001$). RA spasm was observed in 83 patients (11.2 %), and more frequently in patients with anatomical variation than in those with normal anatomy (35.3 % vs 8.7 %, $P < 0.001$). Anatomical variation (OR 4.74; 95 % CI 2.61–8.47; $P < 0.001$) and female gender (OR 2.23; 95 % CI 1.01–4.73; $P = 0.041$) were distinct predictors of RA spasm. Anatomical variations were observed in 9.1 % of the patients, and strongly correlated with RA spasm and procedural achievement of TRCC.

Keywords Radial artery · Transradial approach · Vascular access · Spasm

Introduction

Cardiac catheterization is an essential diagnostic and therapeutic method in evaluating cardiac disease. In recent years, the radial artery (RA) has been considered a safe and useful vascular access site for cardiac catheterization in comparison with the conventional transfemoral approach [1–4]. In general, access-site complications are significantly lower in the transradial approach than in the transfemoral approach. Furthermore, transradial cardiac catheterization (TRCC) shortens hospital stay and improves postprocedure quality of care [5, 6]. The RA has also been considered a reasonable alternative to the saphenous vein graft in coronary artery bypass surgery [7, 8].

However, TRCC also has unique technical challenges, such as access difficulty related to anatomical variations [9–11], RA spasm [12–15], and RA occlusion [16, 17]. Anatomical variations of the RA, such as abnormal RA origin, radioulnar loop, tortuous configuration, and severe RA spasm, occasionally lead to procedural failure. Some previous studies reported that the frequency of anatomical variations of the RA may differ between Asian and Western populations [11, 18]. Furthermore, there is a paucity of data on the relationship between RA spasm and anatomical variations. Thus, we investigated the incidence of anatomical variations of the RA and whether they would affect RA spasm and procedural achievement of TRCC.

Y. Numasawa (✉) · A. Kawamura · S. Kohsaka · M. Takahashi · A. Endo · T. Arai · Y. Ohno · S. Yuasa · Y. Maekawa · K. Fukuda
Department of Cardiology, Keio University School of Medicine, 35 Shinanomachi, Shinjuku-ku, Tokyo 160-8582, Japan
e-mail: numasawa@cpnet.med.keio.ac.jp

Published online: 21 February 2013

Patients and methods

Study population

This was a single-center, prospective study in Japan. This study included 756 consecutive patients with normal Allen test results who underwent TRCC from January 2009 to April 2011. Exclusion criteria were absence of a radial pulse, abnormal Allen test results, and patients undergoing hemodialysis. Patients' characteristics, RA anatomy, RA diameter, and procedural outcomes including spasm were assessed.

Transradial procedure

After local subcutaneous anesthesia with 2 % lidocaine, the RA was punctured with a 20-gauge needle, and a 16-cm hydrophilic-coated sheath (Terumo, Japan) was inserted with gentle manipulation. The size of the sheath was selected at the discretion of the operator. Basically, a 4-F or 5-F sheath was used for diagnostic coronary angiography, and a 6-F sheath was used for coronary intervention. After sheath insertion, 1 mg of isosorbide dinitrate and 5000 IU of heparin were administered through the sheath to prevent RA spasm and thrombotic complications. After administration of isosorbide dinitrate and heparin, retrograde radial arteriography around the elbow joint via a 16-cm sheath was performed in anteroposterior projection to evaluate the RA anatomy from the edge of the sheath to the mid portion of the brachial artery and the RA diameter. We injected half-diluted contrast to prevent contrast-induced spasm. When the transradial procedure failed, it was at the discretion of the operator to attempt the contralateral RA approach, transbrachial approach, or transfemoral approach. Additional doses of heparin were provided based on an ACT level of >300 s during percutaneous coronary intervention (PCI). After the procedure, the arterial sheath was removed immediately and a TR band (Terumo, Tokyo, Japan) was applied for hemostasis in all patients.

Definition of anatomical variations

In this study, anatomical variations of the RA were defined as abnormal origin of the RA and/or radioulnar loop and/or tortuous configuration [9–11, 16, 19]. The RA normally originated from the brachial artery at the level of the

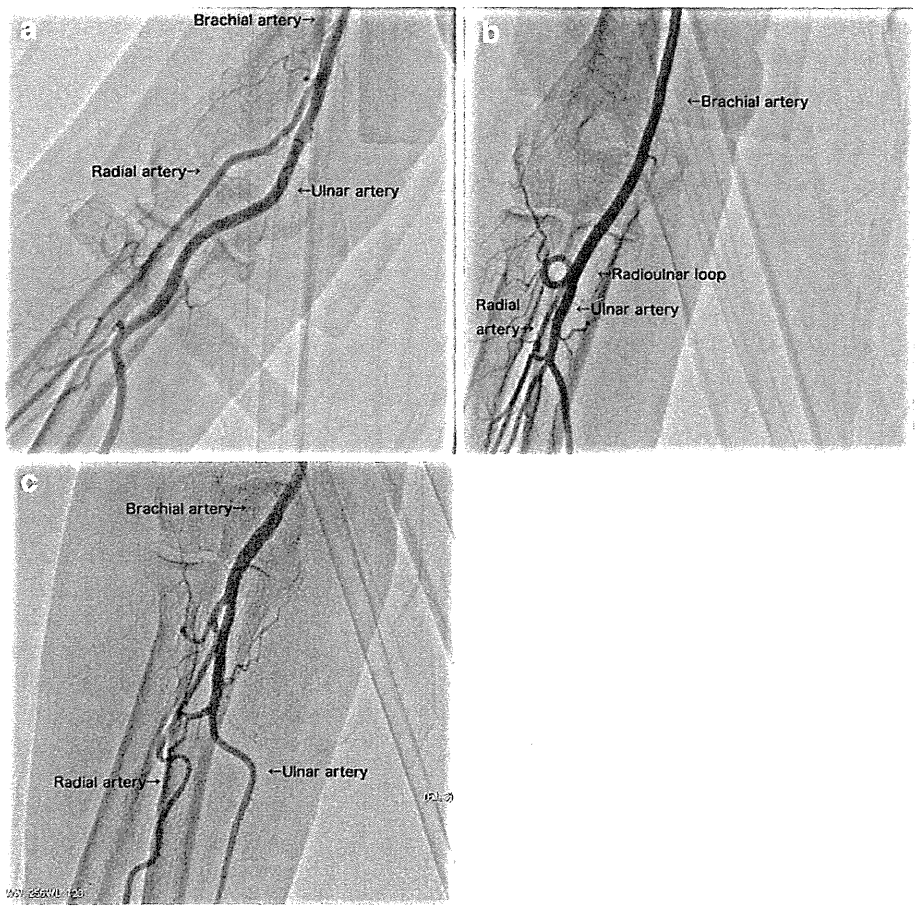

Fig. 1 Anatomical variations of the radial artery, defined as an abnormal origin of the radial artery (**a**) and/or radioulnar loop (**b**) and/or a tortuous configuration of >90° (**c**)

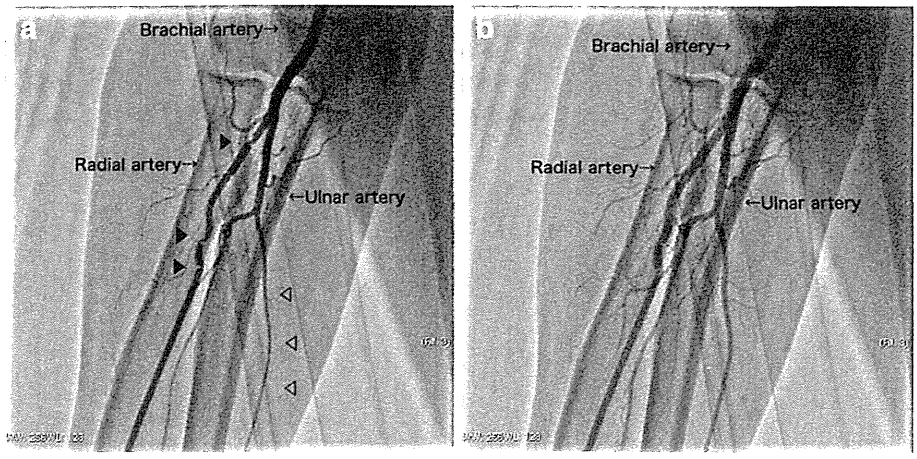

Fig. 2 Radial artery spasm, defined as >75 % stenosis (*black arrowheads*) at first radial arteriography after administration of isosorbide dinitrate and heparin (**a**). The ulnar artery was also diffusely spastic in this case (*white arrowheads*). Arterial spasm was ameliorated after additional administration of isosorbide dinitrate (**b**)

antecubital fossa. Forearm arterial patterns were classified by Uglietta and Kadir [20]. The site of abnormal origin was determined relative to the intercondylar line of the humerus. This line represented the proximal border of the antecubital fossa. Bifurcation of the brachial artery proximal to this line was considered to be the abnormal origin of the RA (Fig. 1a). A radioulnar loop was defined as the presence of a full 360° loop of the RA distal to the bifurcation of the brachial artery (Fig. 1b). Tortuous configuration of the RA was defined as the presence of maximum angulation of >90° (Fig. 1c).

Definition of RA spasm

Radial artery spasm was defined as >75 % stenosis at first radial arteriography after administration of isosorbide dinitrate and heparin [12] (Fig. 2a, b).

Measurement of RA diameter

Proximal RA diameters of the patients were measured at a point 2 cm proximal from the sheath edge. Radial arteriograms were quantitated using the computer-based quantitative coronary angiography (QCA) system Centricity CA1000 (GE Healthcare, Burlington, VT, USA). The outer diameter of the arterial sheath was used for calibration purposes. The outer diameters of the 4-, 5-, and 6-F sheaths (Terumo, Japan) were 1.86, 2.20, and 2.48 mm, respectively. The ratio of sheath outer diameter to RA inner diameter was calculated to measure the RA diameter.

Data analysis

JMP version 8.0 (SAS Institute, Cary, NC, USA) was used for statistical analysis of the data. Continuous variables were expressed as mean and standard deviation (SD). Categorical variables were expressed as a percentage. Continuous variables were compared using Student's *t* test, and the differences between categorical variables were examined using the Chi-square test. Multivariate logistic regression was performed to evaluate the distinct predictors of transradial procedure failure and RA spasm. A *P* value of less than 0.05 was considered statistically significant.

Results

Study population and clinical characteristics

The baseline clinical characteristics of the 756 patients are expressed in Table 1. Mean age was 67.6 ± 11.5 years, and 632 cases (83.6 %) were male. RA puncture was unsuccessful in 12 of 756 cases (1.6 %). Routine retrograde radial arteriography was obtained in 744 cases. PCI was performed in 202 patients (26.7 %). A total of 93.4 % of procedures were attempted via the right RA, and 54.4 % of the procedures were performed using a 5-F sheath.

Anatomical variations of the RA

Overall, anatomical variations of the RA were noted in 68 patients (9.1 %). There were 39 cases of abnormal origin of the RA (5.2 %), 11 cases of radioulnar loop (1.5 %), and 42 cases of tortuous configuration (5.6 %). Patients with abnormal origin of the RA or radioulnar loop frequently had tortuous configuration (33.3 % and 72.7 %, respectively). Six cases had both abnormal origin of the RA and radioulnar loop. The baseline clinical characteristics of patients with anatomical variation and patients with normal anatomy are expressed in Table 2. Patients with anatomical variation were slightly older (70.8 ± 10.7 vs 67.3 ± 11.4 years, $P = 0.017$), shorter (161.1 ± 9.0 vs 164.4 ± 8.1 cm, $P = 0.002$), and lighter (61.8 ± 11.9 vs 65.6 ± 12.4 kg, $P = 0.015$) than patients with normal anatomy. There were

Table 1 Baseline clinical and procedural characteristics of the 756 patients

Age (years)	67.6 ± 11.5
Male	632 (83.6)
Height (cm)	164.0 ± 8.3
Body weight (kg)	65.2 ± 12.4
Body mass index (kg/m^2)	24.1 ± 3.6
Risk factors	
Hypertension	558 (73.8)
Hyperlipidemia	495 (65.5)
Diabetes mellitus	271 (35.8)
Smoking	172 (22.8)
Family history of CAD	119 (15.7)
Serum creatinine (mg/dl)	0.96 ± 0.28
Initial approach	
Right RA	706 (93.4)
Left RA	50 (6.6)
RA puncture failure	12 (1.6)
PCI	202 (26.7)
Sheath size	
4 F	69 (9.1)
5 F	411 (54.4)
6 F	276 (36.5)
Change approach site	38 (5.0)
RA to FA	22 (2.9)
RA to BA	12 (1.6)
RA to contralateral RA	4 (0.5)

Values are presented as *n* (%) or mean ± SD unless otherwise noted
CAD coronary artery disease, *RA* radial artery, *PCI* percutaneous coronary intervention, *FA* femoral artery, *BA* brachial artery

Table 2 Clinical characteristics of the patients with anatomical variation of the radial artery and patients with normal anatomy

	Anatomical variation (+), *n* = 68	Anatomical variation (−), *n* = 676	*P* value
Age (years)	70.8 ± 10.7	67.3 ± 11.4	0.017
Male	43 (63.2)	582 (86.1)	<0.001
Height (cm)	161.1 ± 9.0	164.4 ± 8.1	0.002
Body weight (kg)	61.8 ± 11.9	65.6 ± 12.4	0.015
Body mass index (kg/m^2)	23.7 ± 3.6	24.2 ± 3.6	0.305
Hypertension	46 (67.7)	503 (74.4)	0.247
Hyperlipidemia	43 (63.2)	445 (65.8)	0.689
Diabetes mellitus	22 (32.4)	246 (36.4)	0.596
Smoking	15 (22.1)	155 (22.9)	1.000
Family history of CAD	12 (17.7)	105 (15.5)	0.604
Serum creatinine (mg/dl)	0.99 ± 0.32	0.96 ± 0.27	0.407
Transradial procedure failure	16 (23.5)	10 (1.5)	<0.001
RA spasm	24 (35.3)	59 (8.7)	<0.001

Values are presented as *n* (%) or mean ± SD unless otherwise noted
CAD coronary artery disease, *RA* radial artery

no statistically significant differences in coronary risk factors between patients with anatomical variation and patients with normal anatomy. Details of anatomical variations between males and females are expressed in Table 3. Females had a higher frequency of anatomical variations compared with males (21.0 % vs 6.9 %, $P < 0.001$), especially those with radioulnar loop (5.9 % vs 0.6 %, $P < 0.001$) and tortuous configuration (15.1 % vs 3.8 %, $P < 0.001$). Anatomical variations were frequently related to the transradial procedure failure rate (16 of 68 cases, 23.5 %) and RA spasm (24 of 68 cases, 35.3 %).

Transradial procedure failure

Transradial procedure failure was observed in 26 of 744 cases (3.5 %), and more frequently in patients with anatomical variation of the RA than in patients with normal anatomy (23.5 % vs 1.5 %, $P < 0.001$). The baseline clinical characteristics of these patients are expressed in Table 4. The approach in 18 cases was changed to the femoral artery, and the approach in 8 cases was changed to the brachial artery because of failure of the initial RA approach. The reason for transradial procedure failure included inability to advance the guide wire or catheter in 21 cases (2.8 %) and necessity for a larger sheath or catheter >6 F for PCI in 5 cases (0.7 %). Multivariate logistic regression analysis revealed that the presence of anatomical variation of the RA was the distinct predictor of transradial procedure failure (odds ratio [OR], 17.80; 95 % confidence interval [CI], 7.55–43.73; $P < 0.001$), while age, gender, and short stature (height <155 cm) were not statistically independent predictors after adjustment (Table 5). The procedure failure rate with each of the individual anatomical variations is expressed in Table 6. Each of the variations was associated with transradial procedure failure. Of the anatomical variations, the presence of a radioulnar loop was strongly associated with the highest rate of procedure failure in 8 of the 11 cases (72.7 %, $P < 0.001$).

RA spasm

The baseline clinical characteristics of patients with and without RA spasm are expressed in Table 7. Although routine radial arteriography was performed after administration of isosorbide dinitrate and heparin, RA spasm was

Table 3 Details of anatomical variations of the radial artery between males and females

	Total (n = 744)	Male (n = 625)	Female (n = 119)	P value
Anatomical variation (+)	68 (9.1)	43 (6.9)	25 (21.0)	<0.001
Abnormal origin of the RA	39 (5.2)	27 (4.3)	12 (10.1)	0.021
Radioulnar loop	11 (1.5)	4 (0.6)	7 (5.9)	<0.001
Tortuous configuration	42 (5.6)	24 (3.8)	18 (15.1)	<0.001

Values are presented as n (%)

RA radial artery

Table 4 Clinical characteristics of patients with transradial procedure failure and procedure success

	Procedure failure, n = 26	Procedure success, n = 718	P value
Age (years)	71.5 ± 12.6	67.5 ± 11.4	0.075
Male	17 (65.4)	608 (84.7)	0.024
Height (cm)	159.8 ± 6.9	164.2 ± 8.2	0.008
Body weight (kg)	59.1 ± 12.7	65.5 ± 12.3	0.010
Body mass index (kg/m^2)	23.0 ± 3.9	24.2 ± 3.6	0.113
Hypertension	18 (69.2)	531 (74.0)	0.650
Hyperlipidemia	18 (69.2)	470 (65.5)	0.835
Diabetes mellitus	9 (34.6)	259 (36.1)	1.000
Smoking	4 (15.4)	166 (23.1)	0.478
Family history of CAD	3 (11.5)	114 (15.9)	0.784
Serum creatinine (mg/dl)	1.00 ± 0.27	0.96 ± 0.28	0.466
Anatomical variation	16 (61.5)	52 (7.2)	<0.001
RA spasm	10 (38.5)	73 (10.2)	<0.001

Values are presented as n (%) or mean ± SD unless otherwise noted

CAD coronary artery disease, *RA* radial artery

Table 5 Multivariate logistic regression analysis on transradial procedure failure

	OR	95 % CI	P value
Anatomical variation (+)	17.80	7.55–43.73	<0.001
Age >75 years	2.04	0.83–4.97	0.117
Female gender	1.28	0.34–4.25	0.703
Height <155 cm	1.11	0.27–4.41	0.879

OR odds ratio, *CI* confidence interval

observed in 83 cases (11.2 %), and more frequently in patients with anatomical variation of the RA than in patients with normal anatomy (35.3 % vs 8.7 %, P < 0.001). Females had a higher frequency of RA spasm compared with males (24.4 % vs 8.6 %, P < 0.001). Multivariate logistic regression analysis revealed that the presence of anatomical variation (OR 4.74; 95 % CI 2.61–8.47; P < 0.001) and female gender (OR 2.23; 95 % CI 1.01–4.73; P = 0.041) were the distinct predictors of RA spasm, while use of a 6-F sheath and short stature (height <155 cm) were not statistically independent predictors after adjustment (Table 8).

Table 6 Transradial procedure failure rate in patients with each of the anatomical variations of the radial artery

	n	Procedure failure rate, n (%)	P value
Total	744	26 (3.5)	
Anatomical variation (+)	68	16 (23.5)	<0.001
Abnormal origin of the RA	39	8 (20.5)	<0.001
Radioulnar loop	11	8 (72.7)	<0.001
Tortuous configuration	42	11 (26.2)	<0.001

RA radial artery

RA diameter

Radial artery diameter was analyzed in 701 patients by an angiographic method. Of 744 cases, 43 were excluded from the analysis using the QCA system because of poor angiographic image quality. Mean RA diameter was 2.69 ± 0.37 mm, and was significantly correlated with gender and presence of anatomical variation of the RA. Females had smaller RA diameters than did males (2.40 ± 0.26 vs 2.75 ± 0.36 mm, P < 0.001) (Fig. 3a). Furthermore, patients with anatomical variation of the RA had smaller diameters than did patients with normal anatomy in both males (2.51 ± 0.31 vs 2.77 ± 0.36 mm, P < 0.001) (Fig. 3b) and females (2.24 ± 0.16 vs 2.44 ± 0.26 mm, P < 0.001) (Fig. 3c).

Discussion

The major findings from this study show that anatomical variations of the RA were strongly correlated with RA spasm and procedural achievement of TRCC. It was reported that the procedure success rate of the transradial approach is lower compared with that of the conventional

Table 7 Clinical characteristics of patients with and without radial artery spasm

	Radial artery spasm (+), $n = 83$	Radial artery spasm (−), $n = 661$	*P* value
Age (years)	68.5 ± 11.5	67.5 ± 11.4	0.436
Male	54 (65.1)	571 (86.4)	<0.001
Height (cm)	160.8 ± 9.9	164.5 ± 7.9	<0.001
Body weight (kg)	62.2 ± 14.4	65.6 ± 12.1	0.018
Body mass index (kg/m^2)	23.8 ± 3.8	24.2 ± 3.5	0.426
Hypertension	59 (71.1)	490 (74.1)	0.596
Hyperlipidemia	51 (61.5)	437 (66.1)	0.394
Diabetes mellitus	23 (27.7)	245 (37.1)	0.114
Smoking	20 (24.1)	150 (22.7)	0.782
Family history of CAD	14 (16.9)	103 (15.6)	0.750
Serum creatinine (mg/dl)	0.92 ± 0.27	0.97 ± 0.28	0.145
Transradial procedure failure	10 (12.1)	16 (2.4)	<0.001
Anatomical variation	24 (28.9)	44 (6.7)	<0.001
Use of 6-F sheath	32 (38.6)	241 (36.5)	0.718

Values are presented as *n* (%) or mean ± SD unless otherwise noted

CAD coronary artery disease

transfemoral approach [3]. Thus, it is necessary to elucidate what caused the failure of the transradial approach and identify predictors for a successful transradial approach.

Anatomical variations of the RA and transradial procedure failure

In this study, the incidence of anatomical variations of the RA was 9.1 % (68 of 744 cases), including 39 cases of abnormal origin of the RA (5.2 %), 11 cases of radioulnar loop (1.5 %), and 42 cases of tortuous configuration (5.6 %). The incidence of abnormal origin of the RA, radioulnar loop, and tortuous configuration has been reported to range from 2.4 % to 8.3 %, 0.8 % to 2.3 %, and 2.0 % to 5.2 %, respectively [9–11, 16, 19]. We obtained similar results in the present study. Based on previous reports and the results of our study, it should be recognized that anatomical variations of the RA are not rare beyond those associated with race.

More importantly, in 16 of the 68 patients (23.5 %) with anatomical variations, we failed to perform TRCC as the initial approach. As a result, the procedure success rate was significantly lower in patients with anatomical variation than in patients with normal anatomy (76.5 % vs 98.5 %, $P < 0.001$). Multivariate logistic regression analysis revealed that the presence of anatomical variation was the

Table 8 Multivariate logistic regression analysis on radial artery spasm

	OR	95 % CI	*P* value
Anatomical variation (+)	4.74	2.61–8.47	<0.001
Use of 6-F sheath	1.18	0.71–1.93	0.518
Female gender	2.23	1.01–4.73	0.041
Height <155 cm	1.37	0.59–3.14	0.463

OR odds ratio, *CI* confidence interval

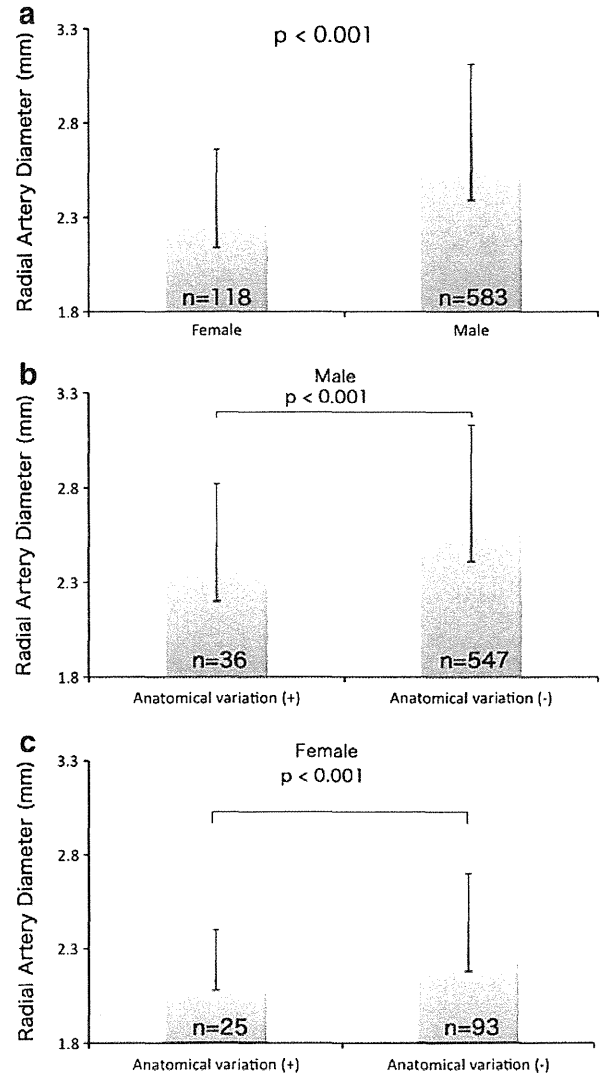

Fig. 3 Differences in radial artery diameter. Proximal radial artery diameter was analyzed in 701 patients by an angiographic method. Females had a smaller radial artery than did males (2.40 ± 0.26 vs 2.75 ± 0.36 mm, $P < 0.001$) (**a**). Patients with anatomical variation of the RA had smaller diameters than did patients with normal anatomy in both males (2.51 ± 0.31 vs 2.77 ± 0.36 mm, $P < 0.001$) (**b**) and females (2.24 ± 0.16 vs 2.44 ± 0.26 mm, $P < 0.001$) (**c**)

distinct predictor of transradial procedure failure. Of the anatomical variations, radioulnar loop was strongly associated with the highest procedural failure rate in 8 of the 11 cases (72.7 %, $P < 0.001$). The transradial procedure failure rate in patients with anatomical variation has been reported to range from 6.9 % to 14.2 % [9, 10, 16]. In our study, it was higher than those reported previously. These differences might be due to differences in definitions of anatomical variations, populations' clinical backgrounds and race, and operators' tenacity in performing the transradial procedure. In any case, the transradial procedure failure rate was higher in patients with anatomical variations. Dehghani et al. [21] reported that an age of >75 years, prior coronary artery bypass graft surgery, and short stature are independent predictors of transradial PCI failure. Although the transradial procedure failure rate tended to be higher in older and shorter patients, an age of >75 years and short stature (height <155 cm) were not statistically independent predictors in our study. Furthermore, the presence of an anatomical variation was much more strongly correlated with transradial procedure failure than was age and height. It is not contraindicated to perform TRCC in patients with anatomical variation of the RA. However, we should recognize that different anatomical variations are associated with different transradial procedure failure rates. Some previous studies reported that the presence of a radioulnar loop was the most common cause of transradial procedure failure [9, 10, 22]. We were sometimes able to pass the radioulnar loop with a hydrophilic guide wire, but the procedure could cause vasospasm and pain. According to previous reports and the results of our study, the presence of a radioulnar loop was not suited to the performance of the transradial procedure.

In this study, radial arteriography was performed immediately after sheath insertion and administration of isosorbide dinitrate and heparin. When we had to change the approach site owing to anatomical variation or severe spasm, especially from the RA to the femoral artery or brachial artery, heparinization might have been associated with bleeding complications. From the standpoint of preventing bleeding complications, we should have performed radial arteriography before the administration of heparin.

Fukuda et al. [12] reported that the proximal RA diameter in a Japanese population was 2.72 ± 0.77 mm in males and 2.49 ± 0.36 mm in females. In our study, the proximal RA diameter measured by the QCA system was similar to those reported previously. Interestingly, both male and female patients with anatomical variation of the RA had smaller diameters than did those with normal anatomy. Smaller RA diameter might contribute to puncture failure and severe vasospasm [12, 13]. In general, the RA is easier to palpate at the wrist than is the ulnar artery in most patients. However, in some patients the ulnar artery is particularly strong on palpation, and quite superficial. Some patients with anatomical variation of the RA had a significantly larger ulnar artery than RA (Fig. 1a). In some of these difficult transradial cases with anatomical variation, the transulnar approach might be a safe and useful alternative to the transradial procedure if the reverse Allen test result is normal [23–25].

It is difficult to detect anatomical variations of the RA by physical examination. Ultrasound examination of the RA is an effective and noninvasive method with which to evaluate RA anatomy before the transradial procedure [13, 19]. Yokoyama et al. [19] reported that preprocedural ultrasound examination could be helpful to measure the RA diameter and to exclude patients with inaccessible arteries including radioulnar loop and tortuous configuration, and those at high risk for access failure. In addition, postprocedural ultrasound examination could detect the patency of the RA [19, 23]. Yokoyama et al. [26] also reported that preprocedural ultrasound examination could be useful not only to detect anatomical variations, but also to assess the collateral supply to the hand instead of a modified Allen test. Thus, ultrasound examination of the RA should be considered before the transradial procedure.

RA spasm

In our study, severe RA spasm (>75 % stenosis at first radial arteriography) was observed in 11.2 % of patients despite preadministration of isosorbide dinitrate. Furthermore, patients with anatomical variation tended to have a smaller RA diameter and more frequent RA spasm than did patients with normal anatomy (35.3 % vs 8.7 %, $P < 0.001$). Multivariate logistic regression analysis revealed that the presence of anatomical variation of the RA and female gender were the distinct predictors of RA spasm. The incidence of RA spasm has been reported to range from 3.8 % to >50 % [12–14, 27–29]. The incidence varied because there were differences in premedication and definition of RA spasm. A case report suggested a relationship between severe vasospasm and anatomical variation of the RA [30]; a patient with abnormal origin of the RA had severe vasospasm of the branching point of the distal axillary artery, resulting in entrapment of the catheter. Although there are some reports on RA spasm, there is a paucity of evidence about the relationship between RA spasm and anatomical variations.

Previous studies reported that female gender, younger age, small RA diameter, lower body mass index, diabetes mellitus, and unsuccessful access at first attempt were distinct predictors of RA spasm [13, 14, 29]. In addition, the presence of anatomical variation was a distinct predictor of RA spasm in our study. Ruiz-Salmeron et al. [31] also reported that anatomical variations of the RA were

strongly associated with RA spasm in multivariate analysis (OR 5.1; 95 % CI 2.2–11.4; $P < 0.001$). These results are in accordance with those in our present study. Use of a 6-F sheath was not a distinct predictor of RA spasm in comparison with use of a 4- or 5-F sheath, while the ratio of the RA diameter and sheath outer diameter was reportedly related to RA occlusion [19].

When preprocedural radial arteriography shows anatomical variation of the RA, especially with small diameter or severe vasospasm, good judgment is needed to potentially change the approach site to the contralateral RA, brachial artery, femoral artery, or even ulnar artery [23–25].

Study limitations

A limitation of this study was the lack of follow-up information on RA patency. The lack of the strict criteria for the operator's experience, the lack of independent angiographic evaluation by a core laboratory, and the lack of ultrasound data on RA anatomy were other limitations of the study. Although radial arteriography was performed after administration of isosorbide dinitrate, pain and stimulation of the sheath insertion might have affected the RA spasm, and RA spasm might have affected RA diameter in this study. Ultrasound examination of the RA is an effective noninvasive method with which to evaluate RA anatomy. Radial arteriography seems to be more precise than ultrasound, but further studies are needed to compare these two methods in terms of accuracy.

Conclusions

Anatomical variations of the RA were observed in 9.1 % of patients, and were strongly correlated with RA spasm and procedural achievement of TRCC. From the standpoint of preventing serious complications, preprocedural radial arteriography is a powerful tool with which to provide precise anatomical information. It requires only a very small amount of contrast media and radiation, and helps operators to safely perform transradial procedures.

Conflict of interest No financial support was provided for our study. We have no relationships with industry. We have no commercial or proprietary interest in the submitted article.

References

1. Brueck M, Bandorski D, Kramer W, Wieczorek M, Holtgen R, Tillmanns H (2009) A randomized comparison of transradial versus transfemoral approach for coronary angiography and angioplasty. JACC Cardiovasc Interv 2:1047–1054
2. Achenbach S, Ropers D, Kallert L, Turan N, Krahner R, Wolf T, Garlichs C, Flachskampf F, Daniel WG, Ludwig J (2008) Transradial versus transfemoral approach for coronary angiography and intervention in patients above 75 years of age. Catheter Cardiovasc Interv 72:629–635
3. Agostoni P, Biondi-Zoccai GG, de Benedictis ML, Rigattieri S, Turri M, Anselmi M, Vassanelli C, Zardini P, Louvard Y, Hamon M (2004) Radial versus femoral approach for percutaneous coronary diagnostic and interventional procedures; Systematic overview and meta-analysis of randomized trials. J Am Coll Cardiol 44:349–356
4. Rao SV, Cohen MG, Kandzari DE, Bertrand OF, Gilchrist IC (2010) The transradial approach to percutaneous coronary intervention: historical perspective, current concepts, and future directions. J Am Coll Cardiol 55:2187–2195
5. Mulukutla SR, Cohen HA (2002) Feasibility and efficacy of transradial access for coronary interventions in patients with acute myocardial infarction. Catheter Cardiovasc Interv 57: 167–171
6. Philippe F, Larrazet F, Meziane T, Dibie A (2004) Comparison of transradial vs transfemoral approach in the treatment of acute myocardial infarction with primary angioplasty and abciximab. Catheter Cardiovasc Interv 61:67–73
7. Vasques F, Rainio A, Heikkinen J, Mikkola R, Lahtinen J, Kettunen U, Juvonen T, Biancari F (2011) Off-pump versus on-pump coronary artery bypass surgery in patients aged 80 years and older: institutional results and meta-analysis. Heart Vessels 26 (online first)
8. Nicolini F, Molardi A, Verdichizzo D, Gallazzi MC, Spaggiari I, Cocconcelli F, Budillon AM, Borrello B, Rivara D, Beghi C, Gherli T (2012) Coronary artery surgery in octogenarians: evolving strategies for the improvement in early and late results. Heart Vessels. doi:10.1007/s00380-011-0198-1
9. Lo TS, Nolan J, Fountzopoulos E, Behan M, Butler R, Hetherington SL, Vijayalakshmi K, Rajagopal R, Fraser D, Zaman A, Hildick-Smith D (2009) Radial artery anomaly and its influence on transradial coronary procedural outcome. Heart 95:410–415
10. Valsecchi O, Vassileva A, Musumeci G, Rossini R, Tespili M, Guagliumi G, Mihalcsik L, Gavazzi A, Ferrazzi P (2006) Failure of transradial approach during coronary interventions: anatomic considerations. Catheter Cardiovasc Interv 67:870–878
11. Yoo BS, Yoon J, Ko JY, Kim JY, Lee SH, Hwang SO, Choe KH (2005) Anatomical consideration of the radial artery for transradial coronary procedures: arterial diameter, branching anomaly and vessel tortuosity. Int J Cardiol 101:421–427
12. Fukuda N, Iwahara S, Harada A, Yokoyama S, Akutsu K, Takano M, Kobayashi A, Kurokawa S, Izumi T (2004) Vasospasms of the radial artery after the transradial approach for coronary angiography and angioplasty. Jpn Heart J 45:723–731
13. Jia DA, Zhou YJ, Shi DM, Liu YY, Wang JL, Liu XL, Wang ZJ, Yang SW, Ge HL, Hu B, Yan ZX, Chen Y, Gao F (2010) Incidence and predictors of radial artery spasm during transradial coronary angiography and intervention. Chin Med J (Engl) 123:843–847
14. Varenne O, Jegou A, Cohen R, Empana JP, Salengro E, Ohanessian A, Gaultier C, Allouch P, Walspurger S, Margot O, El Hallack A, Jouven X, Weber S, Spaulding C (2006) Prevention of arterial spasm during percutaneous coronary interventions through radial artery: the SPASM study. Catheter Cardiovasc Interv 68:231–235
15. Kiemeneij F, Vajifdar BU, Eccleshall SC, Laarman G, Slagboom T, van der Wieken R (2003) Evaluation of a spasmolytic cocktail to prevent radial artery spasm during coronary procedures. Catheter Cardiovasc Interv 58:281–284

16. Nie B, Zhou YJ, Li GZ, Shi DM, Wang JL (2009) Clinical study of arterial anatomic variations for transradial coronary procedure in Chinese population. Chin Med J (Engl) 122:2097–2102
17. Kiemeneij F, Laarman GJ, Odekerken D, Slagboom T, van der Wieken R (1997) A randomized comparison of percutaneous transluminal coronary angioplasty by the radial, brachial and femoral approaches: the access study. J Am Coll Cardiol 29: 1269–1275
18. Yang HJ, Gil YC, Jung WS, Lee HY (2008) Variations of the superficial brachial artery in Korean cadavers. J Korean Med Sci 23:884–887
19. Yokoyama N, Takeshita S, Ochiai M, Koyama Y, Hoshino S, Issiki T, Sato T (2000) Anatomic variations of the radial artery in patients undergoing transradial coronary intervention. Catheter Cardiovasc Interv 49:357–362
20. Uglietta JP, Kadir S (1989) Arteriographic study of variant arterial anatomy of the upper extremities. Cardiovasc Intervent Radiol 12:145–148
21. Dehghani P, Mohammad A, Bajaj R, Hong T, Suen CM, Sharieff W, Chisholm RJ, Kutryk MJ, Fam NP, Cheema AN (2009) Mechanism and predictors of failed transradial approach for percutaneous coronary interventions. JACC Cardiovasc Interv 2:1057–1064
22. Louvard Y, Lefevre T (2000) Loops and transradial approach in coronary diagnosis and intervention. Catheter Cardiovasc Interv 51:250–252
23. Aptecar E, Pernes JM, Chabane-Chaouch M, Bussy N, Catarino G, Shahmir A, Bougrini K, Dupouy P (2006) Transulnar versus transradial artery approach for coronary angioplasty: the PCVI-CUBA study. Catheter Cardiovasc Interv 67:711–720
24. Dashkoff N, Dashkoff PB, Zizzi JA Sr, Wadhwani J, Zizzi JA Jr (2002) Ulnar artery cannulation for coronary angiography and percutaneous coronary intervention: case reports and anatomic considerations. Catheter Cardiovasc Interv 55:93–96
25. Knebel AV, Cardoso CO, Correa Rodrigues LH, Sarmento-Leite RE, de Quadros AS, Mascia Gottschall CA (2008) Safety and feasibility of transulnar cardiac catheterization. Tex Heart Inst J 35:268–272
26. Yokoyama N, Takeshita S, Ochiai M, Hoshino S, Koyama Y, Oshima A, Issiki T, Sato T (2000) Direct assessment of palmar circulation before transradial coronary intervention by color Doppler ultrasonography. Am J Cardiol 86:218–221
27. Chen CW, Lin CL, Lin TK, Lin CD (2006) A simple and effective regimen for prevention of radial artery spasm during coronary catheterization. Cardiology 105:43–47
28. Coppola J, Patel T, Kwan T, Sanghvi K, Srivastava S, Shah S, Staniloae C (2006) Nitroglycerin, nitroprusside, or both, in preventing radial artery spasm during transradial artery catheterization. J Invasive Cardiol 18:155–158
29. Rathore S, Stables RH, Pauriah M, Hakeem A, Mills JD, Palmer ND, Perry RA, Morris JL (2010) Impact of length and hydrophilic coating of the introducer sheath on radial artery spasm during transradial coronary intervention: a randomized study. JACC Cardiovasc Interv 3:475–483
30. Kallivalappil SC, Pullani AJ, Abraham B, Kumar MK, Ashraf SM (2008) Entrapment of a transradial angiogram catheter because of severe vasospasm. J Cardiothorac Vasc Anesth 22: 428–430
31. Ruiz-Salmeron RJ, Mora R, Velez-Gimon M, Ortiz J, Fernandez C, Vidal B, Masotti M, Betriu A (2005) Radial artery spasm in transradial cardiac catheterization. Assessment of factors related to its occurrence, and of its consequences during follow-up. Rev Esp Cardiol 58:504–511

Current Topics

Stem Cell Research for Regenerative Medicine/Personalized Medicine

Novel Insights into Disease Modeling Using Induced Pluripotent Stem Cells

Toru Egashira, Shinsuke Yuasa, and Keiichi Fukuda*

Department of Cardiology, Keio University School of Medicine; 35 Shinanomachi, Shinjuku-ku, Tokyo 160–8582, Japan.

Received October 31, 2012

Induced pluripotent stem cell (iPSC) technology has great potential to establish novel therapeutic approaches in regenerative medicine and disease analysis. Although cell therapy using iPSC-derived cells still has many hurdles to overcome before clinical applications, disease analysis using patient-specific iPSCs may be of practical use in the near future. There are several reports that patient-specific iPSC-derived cells have recapitulated the apparent cellular phenotypes of a wide variety of diseases. Moreover, some studies revealed that it could be possible to discover effective new drugs and to clarify disease pathogenesis by examination of patient-specific iPSC-derived cells *in vitro*. We have recently reported that iPSCs can be a diagnostic tool in a patient with a novel mutation. For definitive diagnosis in a patient with long QT syndrome who had an uncharacterized genetic mutation, we succeeded in clarifying the patient's cellular electrophysiologic characteristics and the molecular mechanism underlying the disease phenotype through the multifaceted analyses of patient-specific iPSC-derived cardiomyocytes. In this review, we focus on the conceptual and practical issues in disease modeling using patient-specific iPSCs and discuss future directions in this research field.

Key words induced pluripotent stem cell; disease modeling; cardiovascular disease; long QT syndrome

1. INTRODUCTION

Induced pluripotent stem cells (iPSCs) are defined as artificial pluripotent stem cells that can be generated from somatic cells by introducing reprogramming factors (*e.g.*, *OCT3/4*, *SOX2*, *KLF4*, *c-MYC*, *NANOG*, and *LIN28*).[1,2] The methodology for generating iPSCs has markedly improved and now integration-free iPSCs, without transgene insertion in the host genome, can be obtained using several procedures.[3–7] iPSCs maintain the two essential stem cell characteristics of infinite self-renewal capability and pluripotency, meaning that they can give rise to all cell types of the three germ layers and differentiate in a fashion similar to normal embryogenesis.[8,9]

One of the expectations of iPSCs is the generation of human disease-specific pluripotent stem cells from patients. Such iPSCs, refered to as patient-specific iPSCs, can differentiate into any type of cell including a patient's diseased organ tissue, and the genetic information of patient-specific iPSCs is identical to that of the patient.[10] Therefore we can directly and repetitively analyze diseased cells using patient-specific iPSC-derived cells. Figure 1 shows the conceptual scheme for the utilization of patient-specific iPSCs in clinical practice. To date, many groups have reported that the apparent cellular phenotypes of genetic disorders can be recapitulated in patient-specific iPSC-derived cells *in vitro* (Table 1). Some reports also involved drug screening using iPSCs, resulting in the proposal of novel drug candidates.[11,12] We have recently reported that functional analyses of patient-specific iPSC-derived cardiomyocytes elucidated the molecular mechanism of the disease phenotype in a patient with undiagnosed sporadic long QT syndrome (LQTS).[13] This paper reviews current topics in disease modeling using patient-specific iPSCs and introduces our study as an actual example in this research field.

2. GENERATION OF PATIENT-SPECIFIC iPSCs

Disease Selection Although any type of disease can theoretically be reproduced by patient-specific iPSC-derived cells, in many diseases it appears difficult to recapitulate the phenotype using this technique because of problems related to both the properties of iPSCs and the disease causality. First, the differentiation efficiency of iPSCs into specific cells restricts the category of disease.[14] In terms of the maturity of iPSC-derived cells, it may be easier to to reproduce the phenotype of disease occurring in younger individuals because of the immaturity of iPSC-derived cells.[15] Disease mainly caused by the alteration of epigenetic status due to environmental parameters is not suitable for modeling using iPSCs because the cellular epigenetic information can be partly renewed during the process of reprogramming.[16,17] On the other hand, in disease directly caused by a genetic aberration that is clearly preserved in iPSCs, it is feasible to confirm whether patient-specific iPSC-derived cells can reproduce diseased cellular kinetics. In addition, apparent phenotypes can be determined even at the single-cell level because of the difficulty in organ formation from iPSCs.[18]

Considering those issues comprehensively, the first disease to be analyzed using patient-specific iPSCs should be a monogenetic disorder with severe phenotypes diagnosed in infancy and easily examined with simple methods at the single-cell level. Most studies using patient-specific iPSCs focus on diseases that satisfy such requirements. LQTS was selected by

The authors declare no conflict of interest.

* To whom correspondence should be addressed. e-mail: kfukuda@a2.keio.jp

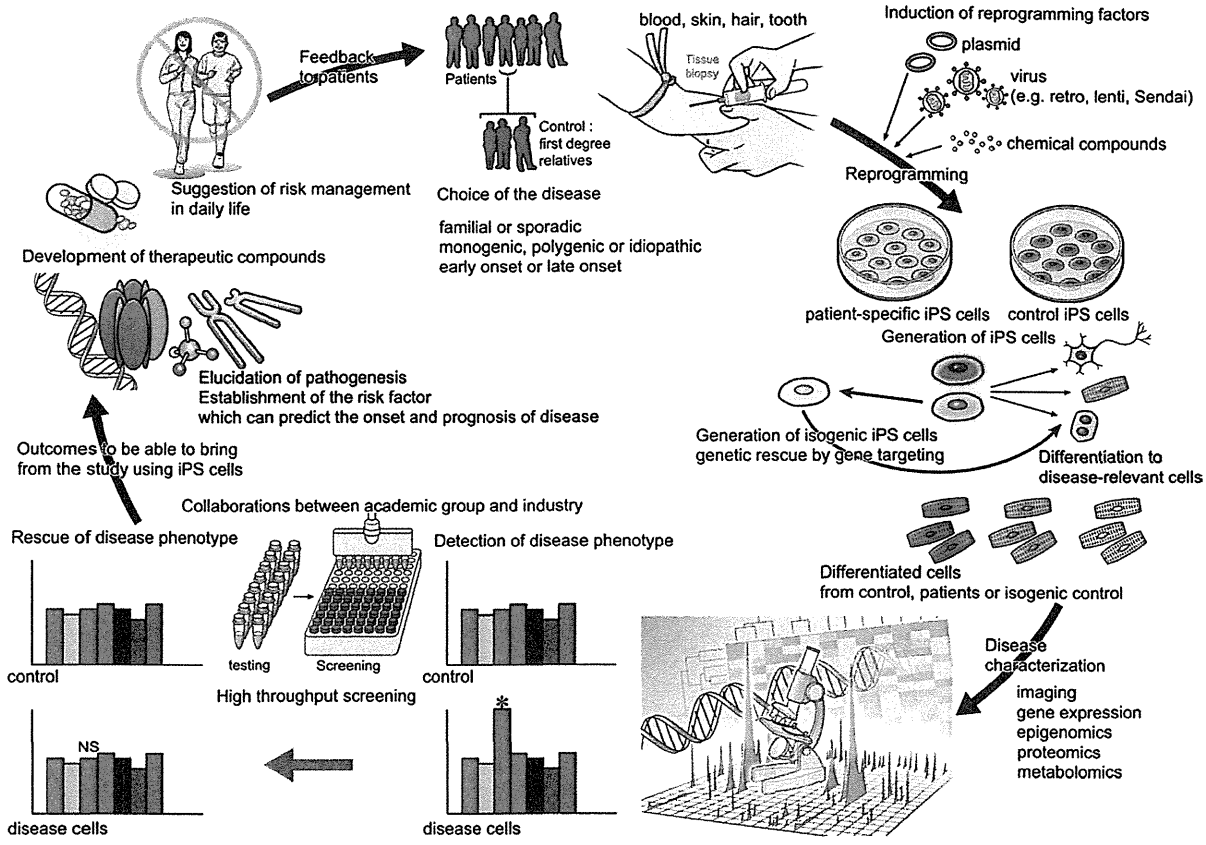

Fig. 1. Overview of Issues in Clinical Applications Using Patient-Specific iPSC Technology

This scheme shows the circle that is one model of patient-specific iPSC technology. The disease type was selected from among many conditions. Controls are often first-degree relatives of patients. Somatic cells are obtained from the blood, skin, hair, or teeth and then reprogramming factors are introduced using various methods (*e.g.*, plasmid, virus, or chemical compounds) and both patient-specific and control iPSCs are generated. If possible, isogenic control iPSCs could be generated through genetic rescue by gene targeting. After evaluating the quality of iPSCs generated, they are differentiated into disease-relevant cells. Then both types of iPSC-derived cell are characterized using various techniques (imaging, genomics, epigenomics, proteomics, metabolomics, *etc.*). Based on the results of pioneering studies, further examinations such as high-throughput screening using large chemical libraries are planned through collaborations between academic research groups and pharmaceutical companies. Expected results of studies on iPSCs are the development of novel therapeutic compounds, establishment of novel risk factors predicting the onset of disease and prognosis, and suggestions on appropriate lifestyles which can serve as feedback to patients.

our and other groups as a disease model using patient-specific iPSCs. LQTS is an inherited life-threatening disease caused by functional impairment of the cardiac ion channel with a monogenetic aberration and often causes sudden cardiac death due to ventricular tachyarrhythmia even in infancy.[19,20]

Derivation and Characterization of Patient-Specific iPSCs Originally, iPSCs were generated from dermal fibroblasts in a retroviral transduction system.[1,21] Subsequently, the methodology for generating iPSCs rapidly improved and became simpler and more efficient, enabling the generation of iPSCs using less patient-invasive methods. Moreover, using plasmid vectors, RNA viruses, and other methods, good-quality iPSCs can be obtained without the need for integrating reprogramming factors.[3–7] Integration-free iPSCs appear ideal because exogenous genes integrated in the host genome may affect the genetic properties of the iPSCs generated and modify the cellular phenotypes of patient-specific iPSC-derived cells.[22]

We previously reported that integration-free iPSCs can be efficiently, easily, and rapidly generated from terminally differentiated circulating T lymphocytes in peripheral blood using Sendai virus (RNA virus).[23] Our method makes it possible to generate iPSCs from any patient including infants, girls, and the very elderly *via* simple blood sampling, which is one of the least-invasive common clinical procedures. Such cumulative progress in generating iPSCs can accelerate the widespread application of patient-specific iPSC technology.

Before the utilization of generated iPSCs in disease modeling, their characteristics must be evaluated.[24] It should be determined whether problems occurred during iPSC reprogramming and maintenance, such as the occurrence of somatic coding mutations,[25] dynamic changes in the allelic copy number variation,[26] abnormality of X chromosome inactivation,[27] incomplete demethylation,[28] *etc.* These elements may affect the phenotype of iPSC-derived cells and skew the interpretation of the results of their assay. In addition, the most appropriate control group remains controversial. In most previous studies, the control groups comprised healthy volunteers without genetic mutations who were unrelated to or relatives of the patients involved. It remains unclear which controls are optimal in disease modeling using patient-specific iPSCs. To examine the unadulterated functions of mutated genes, it appears preferable to compare patients with family members who do not carry the mutation, although related

Table 1. Summary of the Literature on Disease Modeling Using Patient-Specific iPSCs

Disease	Gene mutation	Cell type	Cellular phenotype	Refs.
AD	PS1 mutations	Neurons	Increase in Aβ secretion and rescued by γ-secretase inhibitors	44)
PD	LRRK2 mutations	Neurons-dopaminergic	Degeneration due to increased oxidative-stress	45)
CPVT	RYR2 mutations	Cardiomyocytes	Abnormal dynamism in Ca handling and treatment with several drugs rescues the phenotype	46)
DCM	TNNT2 mutations	Cardiomyocytes	Altered regulation of Ca emphasized by β adrenergic agonist and rescued by β blocker	47)
FH	LDL receptor mutations	Hepatocytes	Impaired ability to incorporate LDL	48)
CML	BCR-ABL	iPSCs, Hematopoietic cells	Imatinib resistant in iPSCs and immature Hematopoietic cells	49)
MD (+DM)	mtDNA A3243G mutation	iPSCs, EBs	Variety of degree of mutation heteroplasmy in each iPSC clones	50)
DS (+AD)	Trisomy 21	Neurons-cortical	Secretion of the pathogenic peptide fragment amyloid-β42	51)
DKC	DKC1, TERT, TCAB1 mutation	iPSCs	Progressive telomere shortening and loss of self-renewal of iPSCs	52), 53)
RP	RP1, RP9, PRPH2, RHO mutations	Rod photoreceptor cells	Decreased numbers of differentiated rod cells and expression of cellular stress markers	54)
GD	GCase mutations	Neurons-dopaminergic	Lysosomal protein degradation, causes accumulation of α-synuclein	55)

AD: Alzheimer's Disease, PD: Parkinson's Disease, CPVT: Catecholaminergic Polymorphic Ventricular Tachycardia, DCM: Dilated Cardiomyopathy, FH: Familial Hypercholesterolemia, CML: Clonic Myeloid Leukemia, MD: Mitochondrial Disease, DM: Diabetes Mellitus, DS: Down Syndrome, DKC: Dyskeratosis Congenita, RP: Retinitis Pigmentosa, GD Gaucher Disease.

family members partly share genetic information including single-nucleotide polymorphisms, and this could affect disease phenotype. A recent study has demonstrated that ideal control iPSCs can be obtained by mutated gene correction using a targeting strategy.[29,30] Even though it cannot be applied in every disease model, further analysis using isogenic-control iPSCs may be the answer to this problem.

Differentiation into Disease Relevant-Cells iPSCs can give rise to a wide variety of cell types present in the three germ layers. In most cases, differentiation methods for iPSCs are applied with some modification from the methods established in embryonic stem cells, which are similar to the regulatory mechanisms of normal early development.[8,9] To establish methods for *in vitro* differentiation from pluripotent stem cells, various screening methods for essential signaling molecules in normal development have been performed.[31]

Among several iPSC lines, the variation in differentiation propensity into specific cell types is well known.[32,33] Therefore the cell type of each iPSC generated should be confirmed before selecting the optimal cell line that can most efficiently differentiate into the cells of interest. A recent study has shown that iPSCs maintain epigenetic memories originally belonging to somatic cells, and this epigenetic status can regulate the characteristics of iPSCs, especially their differentiation propensity.[34–36] Therefore it is important to confirm which cells are the best source for iPSCs to obtain stable, disease-relevant cells.

To investigate more sophisticated experimental conditions similar to the physiologic environment, further improvements are required. First, it is necessary to establish a procedure to purify the cells from aggregations of iPSC-derived miscellaneous cells.[37,38] In addition, it would be ideal to be able to differentiate iPSCs into all constitutive cell types of an organ. In other words, to create organs *in vitro*, not only a single specific cell type but also other cell types such as endothelial cells, fibroblasts, and peripheral neural cells are needed. Furthermore, there are various subpopulations among cardiomyocytes such as atrial-, nodal- and ventricular-type cardiomyocytes, although at present there is no method to obtain each specific cell type.[39] These are crucial limitations on the reliability of results of the novel iPSC assay. In addition, iPSC-derived cells retain the original fetal-like characteristics, and it remains unclear how these cells can be appropriately matured.[40] Still another unresolved issue is the best time in the developmental stage of patient-specific iPSC-derived cells to analyze cellular function in terms of disease properties.

A recent advance in reprogramming to change the cellular fate is direct conversion, which allows terminally differentiated cells to be transformed into other functional cells of different lineages without passing through the pluripotent state.[41,42] In this method, mature target cells can be obtained within a shorter period, and disease modeling using this direct conversion technique has also been reported.[43] However, in spite of lower induction efficiency and the lack of a method established for all cell lineages, iPSCs seem to be a suitable cell source for disease modeling. The infinite self-renewability of iPSCs allows repetitive, reproducible analysis of the disease cells of interest.

Disease Modeling Using Patient-Specific iPSCs To date, several patient-specific iPSC lines have been generated from patients with a wide variety of mainly monogenetic, early-onset diseases such as neurologic disorders,[44,45] heart disease,[46,47] metabolic disease,[48] hematologic disorders,[49] mitochondrial disease,[50] chromosomal abnormalities,[51] telomere disease,[52,53] sensory organ disorder,[54] and storage disease.[55] The current list of studies of disease modeling using patient-specific iPSCs is shown in Table 1. While findings on patient-specific iPSCs have accumulated, analysis becomes more complicated in polygenic, sporadic, late-onset disease.[12,56,57] The next steps that will deliver useful clinical information resulting from patient-specific iPSC technology will result from collaborations between academic research groups and

pharmaceutical companies, which are expected develop novel therapeutic compounds and clarify possible sife effects through advanced high-throughput screening systems using patient-specific iPSC-derived cells.

3. CARDIOVASCULAR DISEASE MODELING USING iPSCs

Functional Characteristics of iPSC-Derived Cardiomyocytes On the premise that the study of human cardiovascular disease modeling will be initiated using patient-specific iPSCs, it is necessary to confirm that the characteristics of human iPSC-derived cardiomyocytes are physiologically analogous to human cardiomyocytes *in vivo*. Previous molecular biological and physiologic studies revealed that iPSC-derived cardiomyocytes have normal cardiomyocyte functional properties.[58,59] iPSC-derived cardiomyocytes have a striated muscle structure identical to that of normal functional cardiomyocytes and express cardiac-specific proteins, as confirmed in molecular biological assays such as immunocytochemistry and reverse-transcriptase polymerase chain reaction (PCR). Based on the waveform of the action potential, iPSC-derived cardiomyocytes can be divided into three subpopulations: atrial, nodal, and ventricular cells. Moreover, the contraction of iPSC-derived cardiomyocytes is regulated by physiologic intracellular signaling including excitation-contraction coupling,[60] and those cardiomyocytes express typical ion channels with the expected functional responses to several ion channel blockers.[61] All these findings indicate the validity of studies that will lead to the analysis of cardiovascular disease using patient-specific iPSC-derived cardiomyocytes.

Modeling LQTS Type 1 Some groups thought that LQTS would be a suitable disease for modeling using iPSCs because of the promising reproducibility of disease phenotypes in iPSC-derived cardiomyocytes.[13,62–67] Moretti *et al.* first showed that patient-specific iPSC-derived cardiomyocytes could recapitulate the disease phenotype in congenital LQTS.[62] They generated iPSCs from two patients with LQTS type 1, who had autosomal-dominant inheritance of a G569A missense mutation in the *KCNQ1* gene encoding the IKs current which was previously shown to be relevant to LQTS onset by functional analysis of the mutated gene.[68]

Individual cardiomyocytes derived from LQTS type 1 patient-specific iPSCs (LQTS1-iPSC-CMs) showed prolonged action potentials using whole-cell patch clamping compared with cardiomyocytes from healthy control donors who were unrelated to the patients. Moreover, LQTS1-iPSC-CMs exhibited increased susceptibility to catecholamine-induced tachyarrhythmia, which is one of the most important clinical features of the syndrome.[69] Even though that study was recognized as an important work first confirming the great potential of patient-specific iPSCs, we thought that there was room for expansion of the scope. In not only that study but also in other reports of LQTS disease modeling using iPSCs, patients who had mutated channel profiles characterized by conventional experimental methods were selected. In reality, many patients have unknown mutations that give no specific information on their disease phenotype. To address whether iPSC technology could be used to characterize the disease phenotype with a novel mutated gene, we selected LQTS patients with no family history or previous disease characterization.[13]

We generated iPSCs from a 13-year-old boy who was a sporadic LQTS patient. He had survived cardiopulmonary arrest due to ventricular fibrillation, and his subtype of LQTS could not be diagnosed using standard clinical tests.[70,71] Two healthy volunteers served as controls who donated iPSCs that had differentiated into cardiomyocytes. Our patient had a novel heterozygous mutation located in the *KCNQ1* gene, 1893delC, identified by genotyping of his blood sample.[72] Electrophysiologic function was measured using a multielectrode array system,[73] which showed that the duration of the field potential was markedly prolonged in LQTS-iPSCs-CMs as compared with cardiomyocytes derived from controls, which suggested that LQTS-iPSC-CMs maintained the patient's characteristics and could be successfully reproduced in this assay system.

Next we tried to confirm the responsible channel for the disease phenotype by precise evaluation of several drug responses. We clarified that the IKs channel was functionally impaired and that the IKr channel could compensate for this effect in LQTS-iPSC-CMs with the administration of several potassium current blockers. In general, the IKr and IKs channels work in a complementary fashion in the repolarization of cardiomyocytes, which is known as the repolarization reserve,[74] and we confirmed that this mechanism regulated the balance of the potassium current in LQTS-iPSC-CMs. Arrhythmogenic events in LQTS-iPSC-CMs caused by adrenergic stimulation also suggested that the patient's IK channel was significantly attenuated.[70,71] These findings strongly suggested that cardiomyocytes in the patient's IKs channel were functionally impaired and that the precise diagnosis was LQTS type 1.[75] To confirm the dominant-negative role of the *KCNQ1* 1893delC mutation in IKs channel function, we performed electrophysiologic and histochemical analyses in iPSC-derived cardiomyocytes and found that *KCNQ1* 1893delC has a dominant-negative effect *via* a trafficking deficiency.

Importantly, our study demonstrated that iPSCs could be useful to characterize the electrophysiologic cellular phenotype of a patient with a novel mutation. We performed functional analysis of the novel mutation using patient-specific iPSCs, which may support the diagnosis of LQTS type 1. Moreover, this system allowed us to perform several drug administration tests on LQTS-iPSC-CMs, which would be extremely risky to such a patient in clinical practice.[76] Therefore patient-specific iPSC technology can be used for drug evaluation and monitoring. At the same time, we were able to clarify the underlying molecular mechanism of the disease phenotype using this assay system.

4. CONCLUSION

Although iPSC technology is an attractive tool for analyzing human genetic diseases, it is clear that technological innovation remains necessary for the utilization of iPSCs in routine medical practice. Disease modeling using patient-specific iPSCs is a novel procedure for analyzing disease. It enables a direct, repetitive approach to diseased cells and has great potential to elucidate novel disease pathogenesis and develop new therapeutic compounds. However, in terms of the effort, cost, and time required in current studies using iPSCs, routine clinical usage is not yet feasible.[77] In addition, improvement of the quality of iPSCs and iPSC-derived cells is required

to make disease models using iPSCs more faithful. Some problems such as genetic mutations during reprogramming, incomplete epigenetic reprogramming, and undesired gene expression should also be controlled and standardized. More sophisticated differentiation, maturation, and purification protocols will be indispensable to create physiologic cellular conditions that reflect the actual disease phenotype.

In conclusion, steady progress is being made in iPSC technology to overcome the hurdles, and disease modeling using iPSCs appears a likely technique for the future. Recent and future innovations in the technique hold out the promise of patient-derived iPSC technology to achieve personalized medicine in the clinical setting.

REFERENCES

1) Takahashi K, Tanabe K, Ohnuki M, Narita M, Ichisaka T, Tomoda K, Yamanaka S. Induction of pluripotent stem cells from adult human fibroblasts by defined factors. *Cell*, **131**, 861–872 (2007).
2) Yu J, Vodyanik MA, Smuga-Otto K, Antosiewicz-Bourget J, Frane JL, Tian S, Nie J, Jonsdottir GA, Ruotti V, Stewart R, Slukvin II, Thomson JA. Induced pluripotent stem cell lines derived from human somatic cells. *Science*, **318**, 1917–1920 (2007).
3) Yu J, Hu K, Smuga-Otto K, Tian S, Stewart R, Slukvin II, Thomson JA. Human induced pluripotent stem cells free of vector and transgene sequences. *Science*, **324**, 797–801 (2009).
4) Kim D, Kim C-H, Moon J-I, Chung YG, Chang MY, Han BS, Ko S, Yang E, Cha KY, Lanza R, Kim KS. Generation of human induced pluripotent stem cells by direct delivery of reprogramming proteins. *Cell Stem Cell*, **4**, 472–476 (2009).
5) Ban H, Nishishita N, Fusaki N, Tabata T, Saeki K, Shikamura M, Takada N, Inoue M, Hasegawa M, Kawamata S, Nishikawa S. Efficient generation of transgene-free human induced pluripotent stem cells (iPSCs) by temperature-sensitive Sendai virus vectors. *Proc. Natl. Acad. Sci. U.S.A.*, **108**, 14234–14239 (2011).
6) Warren L, Manos PD, Ahfeldt T, Loh YH, Li H, Lau F, Ebina W, Mandal PK, Smith ZD, Meissner A, Daley GQ, Brack AS, Collins JJ, Cowan C, Schlaeger TM, Rossi DJ. Highly efficient reprogramming to pluripotency and directed differentiation of human cells with synthetic modified mRNA. *Cell Stem Cell*, **7**, 618–630 (2010).
7) Miyoshi N, Ishii H, Nagano H, Haraguchi N, Dewi DL, Kano Y, Nishikawa S, Tanemura M, Mimori K, Tanaka F, Saito T, Nishimura J, Takemasa I, Mizushima T, Ikeda M, Yamamoto H, Sekimoto M, Doki Y, Mori M. Reprogramming of mouse and human cells to pluripotency using mature microRNAs. *Cell Stem Cell*, **8**, 633–638 (2011).
8) Murry CE, Keller G. Differentiation of embryonic stem cells to clinically relevant populations: lessons from embryonic development. *Cell*, **132**, 661–680 (2008).
9) Irion S, Nostro MC, Kattman SJ, Keller GM. Directed differentiation of pluripotent stem cells: from developmental biology to therapeutic applications. *Cold Spring Harb. Symp. Quant. Biol.*, **73**, 101–110 (2008).
10) Byrne JA. Generation of isogenic pluripotent stem cells. *Hum. Mol. Genet.*, **17** (R1), R37–R41 (2008).
11) Ebert AD, Yu J, Rose FF Jr, Mattis VB, Lorson CL, Thomson JA, Svendsen CN. Induced pluripotent stem cells from a spinal muscular atrophy patient. *Nature*, **457**, 277–280 (2009).
12) Brennand KJ, Simone A, Jou J, Gelboin-Burkhart C, Tran N, Sangar S, Li Y, Mu Y, Chen G, Yu D, McCarthy S, Sebat J, Gage FH. Modelling schizophrenia using human induced pluripotent stem cells. *Nature*, **473**, 221–225 (2011).
13) Egashira T, Yuasa S, Suzuki T, Aizawa Y, Yamakawa H, Matsuhashi T, Ohno Y, Tohyama S, Okata S, Seki T, Kuroda Y, Yae K, Hashimoto H, Tanaka T, Hattori F, Sato T, Miyoshi S, Takatsuki S, Murata M, Kurokawa J, Furukawa T, Makita N, Aiba T, Shimizu W, Horie M, Kamiya K, Kodama I, Ogawa S, Fukuda K. Disease characterization using LQTS-specific induced pluripotent stem cells. *Cardiovasc. Res.*, **95**, 419–429 (2012).
14) Osafune K, Caron L, Borowiak M, Martinez RJ, Fitz-Gerald CS, Sato Y, Cowan CA, Chien KR, Melton DA. Marked differences in differentiation propensity among human embryonic stem cell lines. *Nat. Biotechnol.*, **26**, 313–315 (2008).
15) Dimos JT, Rodolfa KT, Niakan KK, Weisenthal LM, Mitsumoto H, Chung W, Croft GF, Saphier G, Leibel R, Goland R, Wichterle H, Henderson CE, Eggan K. Induced pluripotent stem cells generated from patients with ALS can be differentiated into motor neurons. *Science*, **321**, 1218–1221 (2008).
16) Hochedlinger K, Plath K. Epigenetic reprogramming and induced pluripotency. *Development*, **136**, 509–523 (2009).
17) Meissner A. Epigenetic modifications in pluripotent and differentiated cells. *Nat. Biotechnol.*, **28**, 1079–1088 (2010).
18) Tanaka T, Takahashi K, Yamane M, Tomida S, Nakamura S, Oshima K, Niwa A, Nishikomori R, Kambe N, Hara H, Mitsuyama M, Morone N, Heuser JE, Yamamoto T, Watanabe A, Sato-Otsubo A, Ogawa S, Asaka I, Heike T, Yamanaka S, Nakahata T, Saito MK. Induced pluripotent stem cells from CINCA syndrome patients as a model for dissecting somatic mosaicism and drug discovery. *Blood*, **120**, 1299–1308 (2012).
19) Goldenberg I, Moss AJ. Long QT syndrome. *J. Am. Coll. Cardiol.*, **51**, 2291–2300 (2008).
20) Marbán E. Cardiac channelopathies. *Nature*, **415**, 213–218 (2002).
21) Takahashi K, Yamanaka S. Induction of pluripotent stem cells from mouse embryonic and adult fibroblast cultures by defined factors. *Cell*, **126**, 663–676 (2006).
22) Soldner F, Hockemeyer D, Beard C, Gao Q, Bell GW, Cook EG, Hargus G, Blak A, Cooper O, Mitalipova M, Isacson O, Jaenisch R. Parkinson's disease patient-derived induced pluripotent stem cells free of viral reprogramming factors. *Cell*, **136**, 964–977 (2009).
23) Seki T, Yuasa S, Oda M, Egashira T, Yae K, Kusumoto D, Nakata H, Tohyama S, Hashimoto H, Kodaira M, Okada Y, Seimiya H, Fusaki N, Hasegawa M, Fukuda K. Generation of induced pluripotent stem cells from human terminally differentiated circulating T cells. *Cell Stem Cell*, **7**, 11–14 (2010).
24) Maherali N, Hochedlinger K. Guidelines and techniques for the generation of induced pluripotent stem cells. *Cell Stem Cell*, **3**, 595–605 (2008).
25) Gore A, Li Z, Fung H-L, Young JE, Agarwal S, Antosiewicz-Bourget J, Canto I, Giorgetti A, Israel MA, Kiskinis E, Lee JH, Loh YH, Manos PD, Montserrat N, Panopoulos AD, Ruiz S, Wilbert ML, Yu J, Kirkness EF, Izpisua Belmonte JC, Rossi DJ, Thomson JA, Eggan K, Daley GQ, Goldstein LS, Zhang K. Somatic coding mutations in human induced pluripotent stem cells. *Nature*, **471**, 63–67 (2011).
26) Laurent LC, Ulitsky I, Slavin I, Tran H, Schork A, Morey R, Lynch C, Harness JV, Lee S, Barrero MJ, Ku S, Martynova M, Semechkin R, Galat V, Gottesfeld J, Izpisua Belmonte JC, Murry C, Keirstead HS, Park HS, Schmidt U, Laslett AL, Muller FJ, Nievergelt CM, Shamir R, Loring JF. Dynamic changes in the copy number of pluripotency and cell proliferation genes in human ESCs and iPSCs during reprogramming and time in culture. *Cell Stem Cell*, **8**, 106–118 (2011).
27) Mekhoubad S, Bock C, de Boer AS, Kiskinis E, Meissner A, Eggan K. Erosion of dosage compensation impacts human iPSC disease modeling. *Cell Stem Cell*, **10**, 595–609 (2012).
28) Ohi Y, Qin H, Hong C, Blouin L, Polo JM, Guo T, Qi Z, Downey SL, Manos PD, Rossi DJ, Yu J, Hebrok M, Hochedlinger K, Costello JF, Song JS, Ramalho-Santos M. Incomplete DNA methylation underlies a transcriptional memory of somatic cells in human iPS cells. *Nat. Cell Biol.*, **13**, 541–549 (2011).
29) Soldner F, Laganière J, Cheng AW, Hockemeyer D, Gao Q, Alagappan R, Khurana V, Golbe LI, Myers RH, Lindquist S, Zhang

L, Guschin D, Fong LK, Vu BJ, Meng X, Urnov FD, Rebar EJ, Gregory PD, Zhang HS, Jaenisch R. Generation of isogenic pluripotent stem cells differing exclusively at two early onset Parkinson point mutations. *Cell*, **146**, 318–331 (2011).

30) Ananiev G, Williams EC, Li H, Chang Q. Isogenic pairs of wild type and mutant induced pluripotent stem cell (iPSC) lines from Rett syndrome patients as *in vitro* disease model. *PLoS ONE*, **6**, e25255 (2011).

31) Srivastava D. Making or breaking the heart: from lineage determination to morphogenesis. *Cell*, **126**, 1037–1048 (2006).

32) Hu B-Y, Weick JP, Yu J, Ma LX, Zhang XQ, Thomson JA, Zhang SC. Neural differentiation of human induced pluripotent stem cells follows developmental principles but with variable potency. *Proc. Natl. Acad. Sci. U.S.A.*, **107**, 4335–4340 (2010).

33) Kattman SJ, Witty AD, Gagliardi M, Dubois NC, Niapour M, Hotta A, Ellis J, Keller G. Stage-specific optimization of activin/nodal and BMP signaling promotes cardiac differentiation of mouse and human pluripotent stem cell lines. *Cell Stem Cell*, **8**, 228–240 (2011).

34) Polo JM, Liu S, Figueroa ME, Kulalert W, Eminli S, Tan KY, Apostolou E, Stadtfeld M, Li Y, Shioda T, Natesan S, Wagers AJ, Melnick A, Evans T, Hochedlinger K. Cell type of origin influences the molecular and functional properties of mouse induced pluripotent stem cells. *Nat. Biotechnol.*, **28**, 848–855 (2010).

35) Kim K, Doi A, Wen B, Ng K, Zhao R, Cahan P, Kim J, Aryee MJ, Ji H, Ehrlich LI, Yabuuchi A, Takeuchi A, Cunniff KC, Hongguang H, McKinney-Freeman S, Naveiras O, Yoon TJ, Irizarry RA, Jung N, Seita J, Hanna J, Murakami P, Jaenisch R, Weissleder R, Orkin SH, Weissman IL, Feinberg AP, Daley GQ. Epigenetic memory in induced pluripotent stem cells. *Nature*, **467**, 285–290 (2010).

36) Kim K, Zhao R, Doi A, Ng K, Unternaehrer J, Cahan P, Huo H, Loh YH, Aryee MJ, Lensch MW, Li H, Collins JJ, Feinberg AP, Daley GQ. Donor cell type can influence the epigenome and differentiation potential of human induced pluripotent stem cells. *Nat. Biotechnol.*, **29**, 1117–1119 (2011).

37) Hattori F, Chen H, Yamashita H, Tohyama S, Satoh YS, Yuasa S, Li W, Yamakawa H, Tanaka T, Onitsuka T, Shimoji K, Ohno Y, Egashira T, Kaneda R, Murata M, Hidaka K, Morisaki T, Sasaki E, Suzuki T, Sano M, Makino S, Oikawa S, Fukuda K. Nongenetic method for purifying stem cell-derived cardiomyocytes. *Nat. Methods*, **7**, 61–66 (2010).

38) Dubois NC, Craft AM, Sharma P, Elliott DA, Stanley EG, Elefanty AG, Gramolini A, Keller G. SIRPA is a specific cell-surface marker for isolating cardiomyocytes derived from human pluripotent stem cells. *Nat. Biotechnol.*, **29**, 1011–1018 (2011).

39) Nelson TJ, Martinez-Fernandez A, Terzic A. Induced pluripotent stem cells: developmental biology to regenerative medicine. *Nat. Rev. Cardiol.*, **7**, 700–710 (2010).

40) Blazeski A, Zhu R, Hunter DW, Weinberg SH, Zambidis ET, Tung L. Cardiomyocytes derived from human induced pluripotent stem cells as models for normal and diseased cardiac electrophysiology and contractility. *Prog. Biophys. Mol. Biol.*, **110**, 166–177 (2012).

41) Szabo E, Rampalli S, Risueño RM, Schnerch A, Mitchell R, Fiebig-Comyn A, Levadoux-Martin M, Bhatia M. Direct conversion of human fibroblasts to multilineage blood progenitors. *Nature*, **468**, 521–526 (2010).

42) Ambasudhan R, Talantova M, Coleman R, Yuan X, Zhu S, Lipton SA, Ding S. Direct reprogramming of adult human fibroblasts to functional neurons under defined conditions. *Cell Stem Cell*, **9**, 113–118 (2011).

43) Qiang L, Fujita R, Yamashita T, Angulo S, Rhinn H, Rhee D, Doege C, Chau L, Aubry L, Vanti WB, Moreno H, Abeliovich A. Directed conversion of Alzheimer's disease patient skin fibroblasts into functional neurons. *Cell*, **146**, 359–371 (2011).

44) Koch P, Tamboli IY, Mertens J, Wunderlich P, Ladewig J, Stüber K, Esselmann H, Wiltfang J, Brüstle O, Walter J. Presenilin-1 L166P mutant human pluripotent stem cell-derived neurons exhibit partial loss of γ-secretase activity in endogenous amyloid-β generation. *Am. J. Pathol.*, **180**, 2404–2416 (2012).

45) Nguyen HN, Byers B, Cord B, Shcheglovitov A, Byrne J, Gujar P, Kee K, Schüle B, Dolmetsch RE, Langston W, Palmer TD, Pera RR. LRRK2 mutant iPSC-derived DA neurons demonstrate increased susceptibility to oxidative stress. *Cell Stem Cell*, **8**, 267–280 (2011).

46) Itzhaki I, Maizels L, Huber I, Gepstein A, Arbel G, Caspi O, Miller L, Belhassen B, Nof E, Glikson M, Gepstein L. Modeling of catecholaminergic polymorphic ventricular tachycardia with patient-specific human-induced pluripotent stem cells. *J. Am. Coll. Cardiol.*, **60**, 990–1000 (2012).

47) Sun N, Yazawa M, Liu J, Han L, Sanchez-Freire V, Abilez OJ, Navarrete EG, Hu S, Wang L, Lee A, Pavlovic A, Lin S, Chen R, Hajjar RJ, Snyder MP, Dolmetsch RE, Butte MJ, Ashley EA, Longaker MT, Robbins RC, Wu JC. Patient-specific induced pluripotent stem cells as a model for familial dilated cardiomyopathy. *Sci. Transl. Med.*, **4**, ra47 (2012).

48) Rashid ST, Corbineau S, Hannan N, Marciniak SJ, Miranda E, Alexander G, Huang-Doran I, Griffin J, Ahrlund-Richter L, Skepper J, Semple R, Weber A, Lomas DA, Vallier L. Modeling inherited metabolic disorders of the liver using human induced pluripotent stem cells. *J. Clin. Invest.*, **120**, 3127–3136 (2010).

49) Kumano K, Arai S, Hosoi M, Taoka K, Takayama N, Otsu M, Nagae G, Ueda K, Nakazaki K, Kamikubo Y, Eto K, Aburatani H, Nakauchi H, Kurokawa M. Generation of induced pluripotent stem cells from primary chronic myelogenous leukemia patient samples. *Blood*, **119**, 6234–6242 (2012).

50) Fujikura J, Nakao K, Sone M, Noguchi M, Mori E, Naito M, Taura D, Harada-Shiba M, Kishimoto I, Watanabe A, Asaka I, Hosoda K, Nakao K. Induced pluripotent stem cells generated from diabetic patients with mitochondrial DNA A3243G mutation. *Diabetologia*, **55**, 1689–1698 (2012).

51) Shi Y, Kirwan P, Smith J, MacLean G, Orkin SH, Livesey FJ. A human stem cell model of early Alzheimer's disease pathology in Down syndrome. *Sci. Transl. Med.*, **4**, ra29 (2012).

52) Batista LFZ, Pech MF, Zhong FL, Nguyen HN, Xie KT, Zaug AJ, Crary SM, Choi J, Sebastiano V, Cherry A, Giri N, Wernig M, Alter BP, Cech TR, Savage SA, Reijo Pera RA, Artandi SE. Telomere shortening and loss of self-renewal in dyskeratosis congenita induced pluripotent stem cells. *Nature*, **474**, 399–402 (2011).

53) Agarwal S, Loh Y-H, McLoughlin EM, Huang J, Park IH, Miller JD, Huo H, Okuka M, Dos Reis RM, Loewer S, Ng HH, Keefe DL, Goldman FD, Klingelhutz AJ, Liu L, Daley GQ. Telomere elongation in induced pluripotent stem cells from dyskeratosis congenita patients. *Nature*, **464**, 292–296 (2010).

54) Jin Z-B, Okamoto S, Osakada F, Homma K, Assawachananont J, Hirami Y, Iwata T, Takahashi M. Modeling retinal degeneration using patient-specific induced pluripotent stem cells. *PLoS ONE*, **6**, e17084 (2011).

55) Mazzulli JR, Xu Y-H, Sun Y, Knight AL, McLean PJ, Caldwell GA, Sidransky E, Grabowski GA, Krainc D. Gaucher disease glucocerebrosidase and α-synuclein form a bidirectional pathogenic loop in synucleinopathies. *Cell*, **146**, 37–52 (2011).

56) Israel MA, Yuan SH, Bardy C, Reyna SM, Mu Y, Herrera C, Hefferan MP, Van Gorp S, Nazor KL, Boscolo FS, Carson CT, Laurent LC, Marsala M, Gage FH, Remes AM, Koo EH, Goldstein LS. Probing sporadic and familial Alzheimer's disease using induced pluripotent stem cells. *Nature*, **482**, 216–220 (2012).

57) Cohen JD, Babiarz JE, Abrams RM, Guo L, Kameoka S, Chiao E, Taunton J, Kolaja KL. Use of human stem cell derived cardiomyocytes to examine sunitinib mediated cardiotoxicity and electrophysiological alterations. *Toxicol. Appl. Pharmacol.*, **257**, 74–83 (2011).

58) Tanaka T, Tohyama S, Murata M, Nomura F, Kaneko T, Chen H, Hattori F, Egashira T, Seki T, Ohno Y, Koshimizu U, Yuasa